Waiho River: Change Detection Analysis

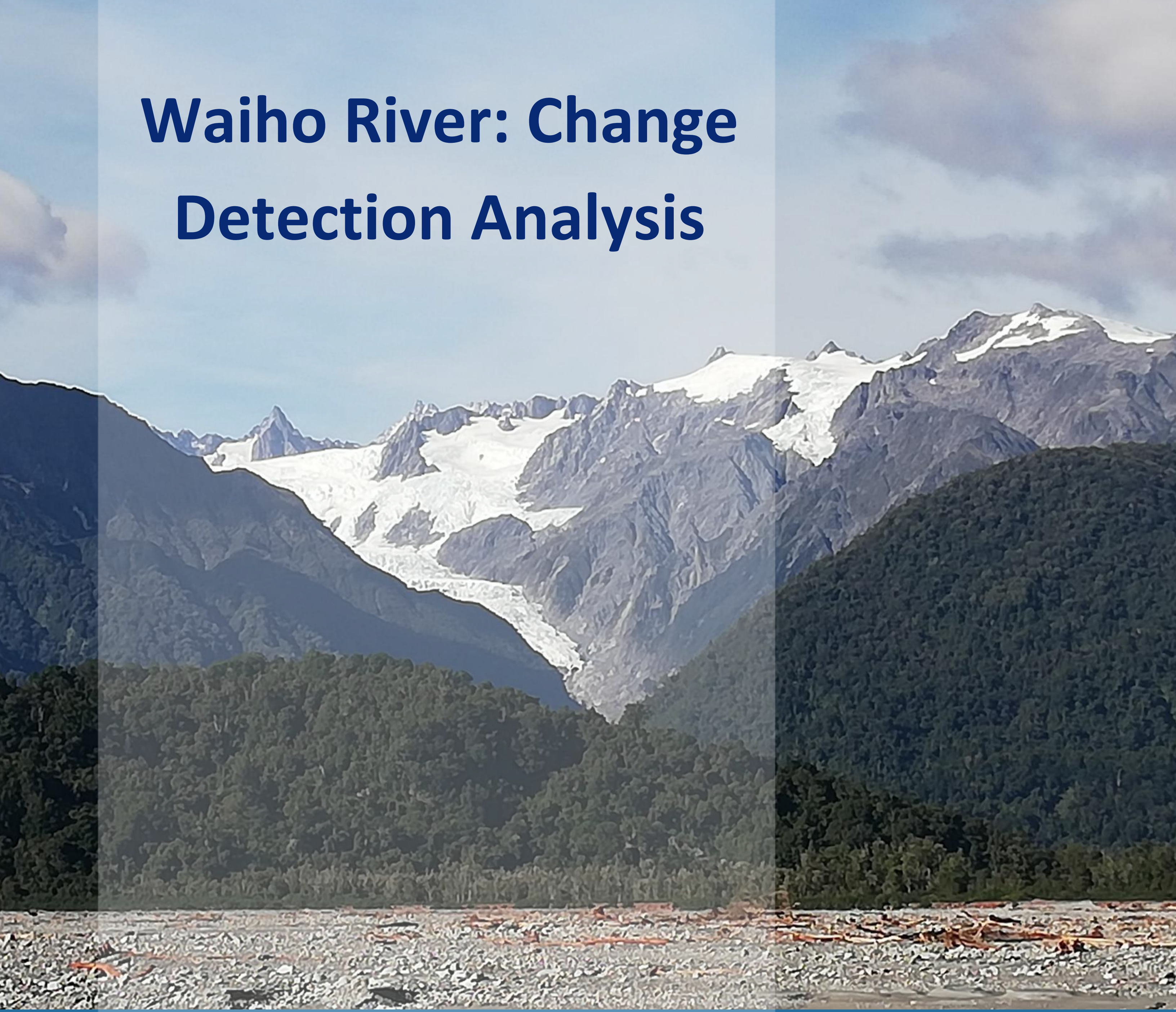

JULY 31, 2019

ANALYSIS OF CHANGE BETWEEN 2016 AND 2019 LIDAR SURVEYS

Client: West Coast Regional Council

Report by: Matthew Gardner & James Brasington

Land River Sea Consulting / Waikato University

www.landriversea.com www.waikato.ac.nz

WAIHO RIVER: CHANGE DETECTION ANALYSIS

REVISION HISTORY

Author:	Matthew Gardner, James Brasington
Signature:	
Date:	31/7/2019
Revision:	01
Authorised by:	Randal Beal
Signature:	
Organisation:	West Coast Regional Council
Date:	

Land River Sea Consulting Limited
5 Achilles Street
Burwood
Christchurch

M: +64 27 318 9527
E: matthew@landriversea.com
W: landriversea.com

TABLE OF CONTENTS

REVISION HISTORY I

1. INTRODUCTION 1

1.1 Objective 1

1.2 Background 1

2. DATA COLLECTION / PREPARATION 3

2016 LiDAR 3

2016 Cross Section Survey 3

2019 LIDAR 3

3. CHANGE DETECTION METHODOLOGY 4

3.1 GCD Software 4

3.2 DEM Uncertainty Modelling 4

3.3 Area of Interest 7

3.4 Sub Reach ANalysis 8

4. RESULTS PRESENTATION 11

4.1 Broadscale Patterns of Bed-Level Change and Channel Adjustment 11

4.2 Cross Sectional Analysis 14

4.3 Longitudinal Analysis BaseD on 500m units 17

5. CROSS SECTION MEAN BED LEVEL ANALYSIS 19

6. DISCUSSIONS 23

6.1 Impact of Weather Patterns on Sedimentation 23

6.2 Future Sedimentation Trends 24

7. CONCLUSIONS 25

8. REFERENCES 26

APPENDIX A – GCD VISUAL REPRESENTATION 27

APPENDIX B – CROSS SECTIONAL MBL COMPARISON 1983 TO 2019 28

1. INTRODUCTION

1.1 OBJECTIVE

Land River Sea Consulting in conjunction with Waikato University have been contracted by the West Coast Regional Council in order to carry out an analysis of the changes in bed levels which have occurred in the Waiho River Catchment between the periods of 2016 and 2019, as well as commenting on the long term bed level trend in relation to historic surveys.

The comparison is primarily to be carried out between LiDAR datasets collected in July 2016 and April 2019, however commentary is also made on the changes in relation to historic cross section surveys going back to 1983.

1.2 BACKGROUND

The Waiho River is located on the West Coast of the South Island of New Zealand, running from the Franz Josef Glacier in the Southern Alps to the Tasman Sea, approximately 10km southwest of Okarito. The river is crossed by the State Highway 6 (SH6) Bridge which is operated by the New Zealand Transport Authority (NZTA) and runs adjacent to the town of Franz Josef / Waiau, situated on the true right bank of the river.

The area has a high level of geologic activity, with the Alpine Fault running through the town of Franz Josef itself and crossing the river in the vicinity of the SH6 Bridge. From the glacier, the Waiho River is confined in a glacial valley, with steep sides. The river is confined in the upper reaches but widens out and has a wide gravel bed downstream of the State Highway Bridge. The river widens out into a natural alluvial fan, however the current fan is constrained on the true left bank by man-made stopbanks, forcing the river to aggrade in its current alignment, rather than naturally deposit sediment over a wider area.

The main tributary of the Waiho River within the study area is the Callery River which enters the Waiho River immediately upstream of SH6. Figure 1-1 shows the location of the Waiho River as well as the catchment boundaries which feed the river within the study area.

Figure 1-1 – Location map of the Waiho River highlighting the hydrological catchments for the Waiho River and the Callery River upstream of SH6 bridge

2. DATA COLLECTION / PREPARATION

2016 LIDAR

LiDAR data was collected in June 2016 by New Zealand Aerial Surveys Ltd. The data was supplied in the form of a 1m DEM as well as with a raw point cloud in LAS format classified into ground and non-ground points.

The data is reported to have been collected using a fixed wing aircraft equipped with an Optech Orion H300 sensor at altitudes between 1190-2375 m

The elevation accuracy of the resulting 3D point cloud was assessed using checkpoint survey observations acquired on bare earth surfaces. The standard deviation of the differences between the checkpoints and locally interpolated point cloud is reported to be 0.016 m and the average difference is 0.007 m suggesting minimal bias.

2016 CROSS SECTION SURVEY

Chris J Coll & Associates carried out a full cross section survey of the Waiho River in April 2016. In order to fully utilise this survey data in this analysis, the water surface has been manually delineated based on the aerial imagery collected at the time of collecting the LiDAR and the wetted channel has been interpolated between cross sections utilising tools within the DHI Mike Hydro River software as well as in ArcGIS. This DEM of the wetted channel has then been merged with the DEM generated from the LiDAR.

2019 LIDAR

LiDAR data was collected in April 2019 by James Brasington from Waikato University. Data was supplied as a 1m DEM as well in with a raw point cloud in LAS format classified into ground and non-ground points.

The data was acquired from a helicopter equipped with a Riegl VUX-1LR sensor at an altitude of 350 m above ground.

The elevation accuracy of the resulting 3D point cloud was assessed using a checkpoint survey of n=97 observations acquired on bare earth surfaces. The standard deviation of the differences between the checkpoints and locally interpolated point cloud was found to 0.017 m and the average difference is 0.001 m with an RMS error of 0.017 m suggesting minimal bias.

3. CHANGE DETECTION METHODOLOGY

3.1 GCD SOFTWARE

The analysis has been undertaken using the Geomorphic Change Detection (GCD, see gcd.riverscapes.xyz) toolkit developed by James Brasington (University of Waikato), Joe Wheaton (Utah State University) and Philip Bailey (North Arrow Research). The GCD toolkit facilitates the measurement of bed level change by comparing time-series of digital elevation models and accounting for the uncertainty that arises from survey instrument errors, interpolation artefacts, surface roughness and the pattern of spatial sampling.

The GCD toolkit uses the statistical theory of errors to enable users to classify the probability that elevation differences observed between two DEMs are likely to be significant (real) relative to the underlying data uncertainty. The method generates a cell-by-cell model of elevation change, termed a Digital Elevation model of Difference (DoD) from which the local patterns of bed level change can be aggregated to yield total and regional areas and volumes of predicted bed level decreases (i.e., erosion, subsidence or sediment extraction) and bed level increase (i.e., sedimentation, uplift or sediment augmentation).

Several methods are available for accounting for DEM uncertainty in a GCD analysis. In this study, the probabilistic thresholding approach is applied. This allows for an estimate of error to be applied separately for each input DEM and then propagates these errors through to a Difference of DEMs (DoD) using standard statistical theory. The GCD tool then compares the propagated error to the observed elevation change on a cell-by-cell basis and evaluates the probability that the change is could be due to chance sampling errors using a 'Students t' score. This approach enables the user to define a statistical threshold – a confidence interval – to filter changes that are assumed to be 'real' and those that reflect uncertainties in the underlying data (Brasington et al., 2003; Wheaton et al., 2010; Vericat et al., 2017).

In the analysis reported here, a sensitivity experiment was used to compare bed level change predictions based on three confidence intervals: 68%, 84% and 95%. Following analysis of the results from each run, here we focus on the 84% confidence interval, to present the overall analysis, though we incorporate results from the additional uncertainty thresholds in the accompanying appendix. The resulting maps presented, and the areas/volumes of change tabulated therefore include only elevation changes that have an 84% or greater likelihood of being significant relative to the underlying data uncertainty.

3.2 DEM UNCERTAINTY MODELLING

A spatial model of DEM uncertainty was constructed for each surface (2016 and 2019) based on the observed pattern of land cover. Given the high quality (low magnitude of vertical errors reported) of the two lidar datasets, the surface cover is first order control on data quality. This reflects the combined effects of vegetation cover on the ability to of the lidar survey to penetrate to through to ground level, the local surface roughness (e.g., riverbed gravels vs pasture) and the effects on laser reflectivity – in particular the lack of data retrievals on wet/inundated areas. To represent these effects, data masks (Figures 3-1 and

3-2) were developed for both the 2016 and 2019 datasets using temporally coincident multispectral satellite imagery from the Sentinel 2 platform. The multispectral data were used to provide an unsupervised classification of the land cover at a 10 m resolution, based on a five-point classification scheme. For each land cover class, an estimated vertical uncertainty was set, guided by the local pattern of elevation uncertainty revealed in the raw point cloud. The resulting land-cover classification and DEM elevation uncertainty is shown in Table 3-1.

Table 3-1 – Land cover classification and associated DEM uncertainty

Land Cover Class	Characteristic Vertical Uncertainty (m)
Exposed river gravels	0.13
Inundated areas (without correction)	0.5
Inundated areas (with section corrections, 2016 only)	0.25
Pasture	0.15
Tall Vegetation	0.3

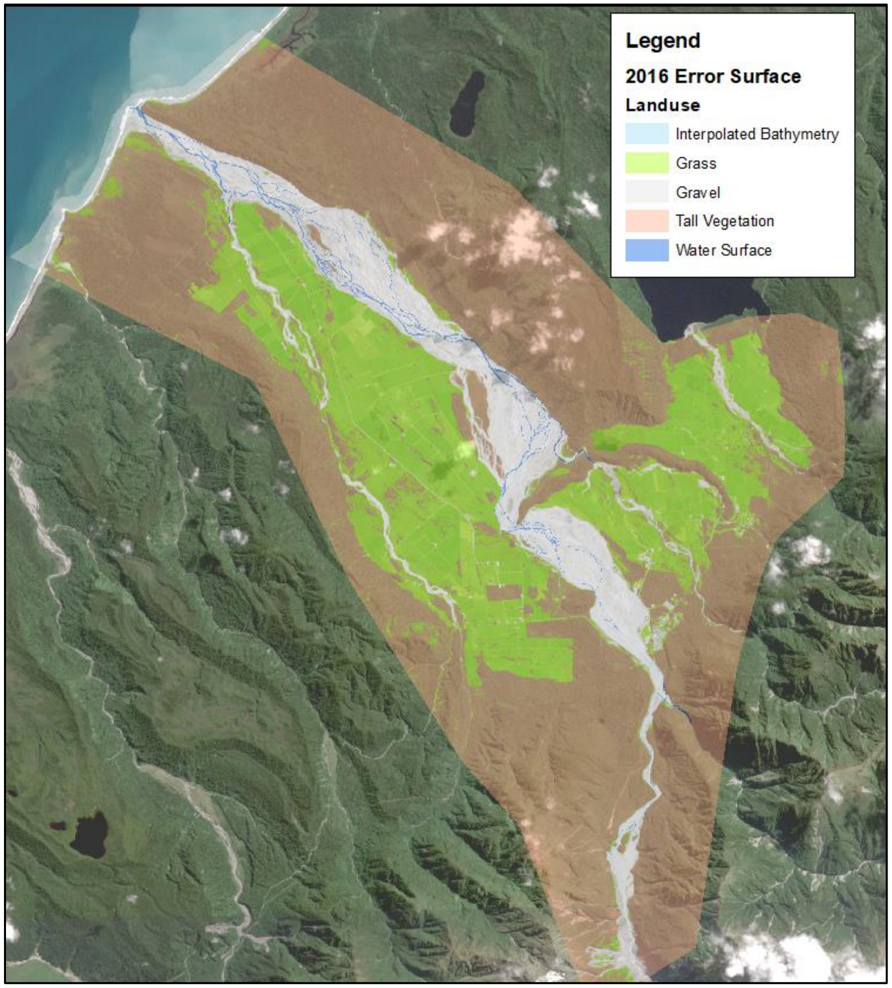

Figure 3-1 – Uncertainty Mask – 2016 LiDAR

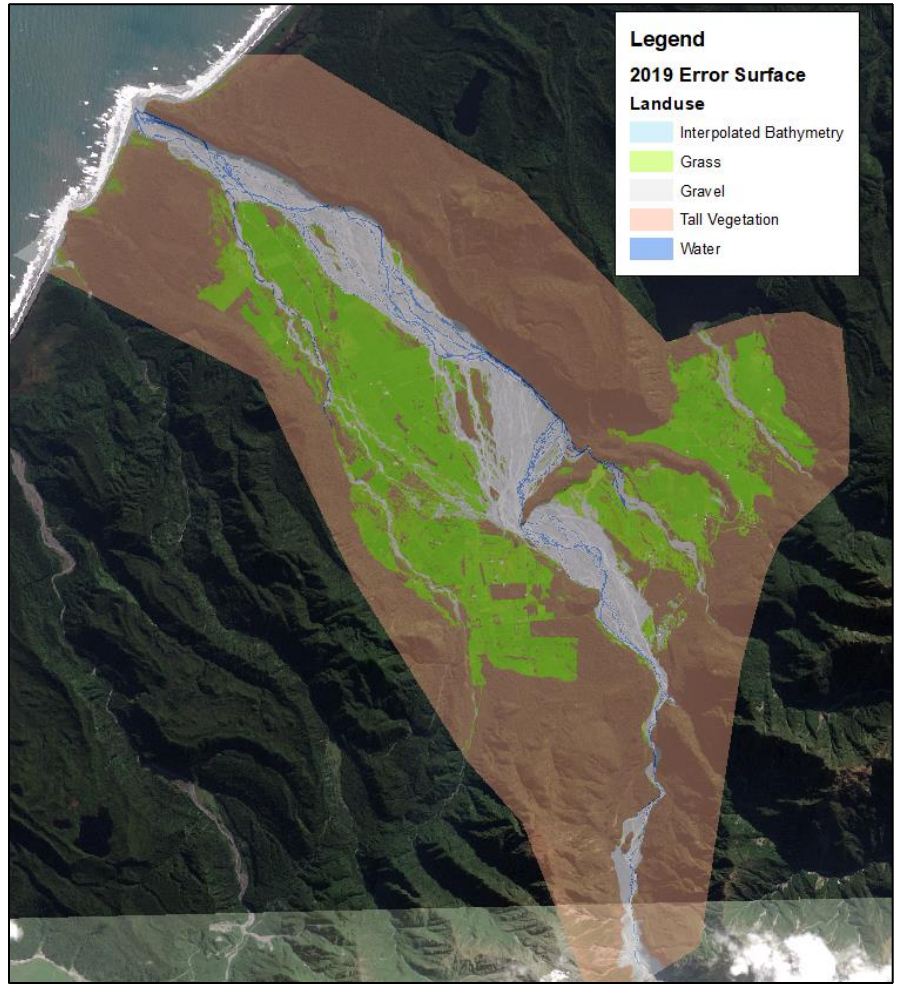

Figure 3-2 - Uncertainty Mask – 2019 LiDAR

3.3 AREA OF INTEREST

The main area of interest for the change analysis has been defined as the active channel of the Waiho River, but has also included a section of the Tartare Stream as well as the outbreak path of the Waiho River downstream from Milton's Bank.

The area of interest used in the analysis is presented in Figure 3-3 below.

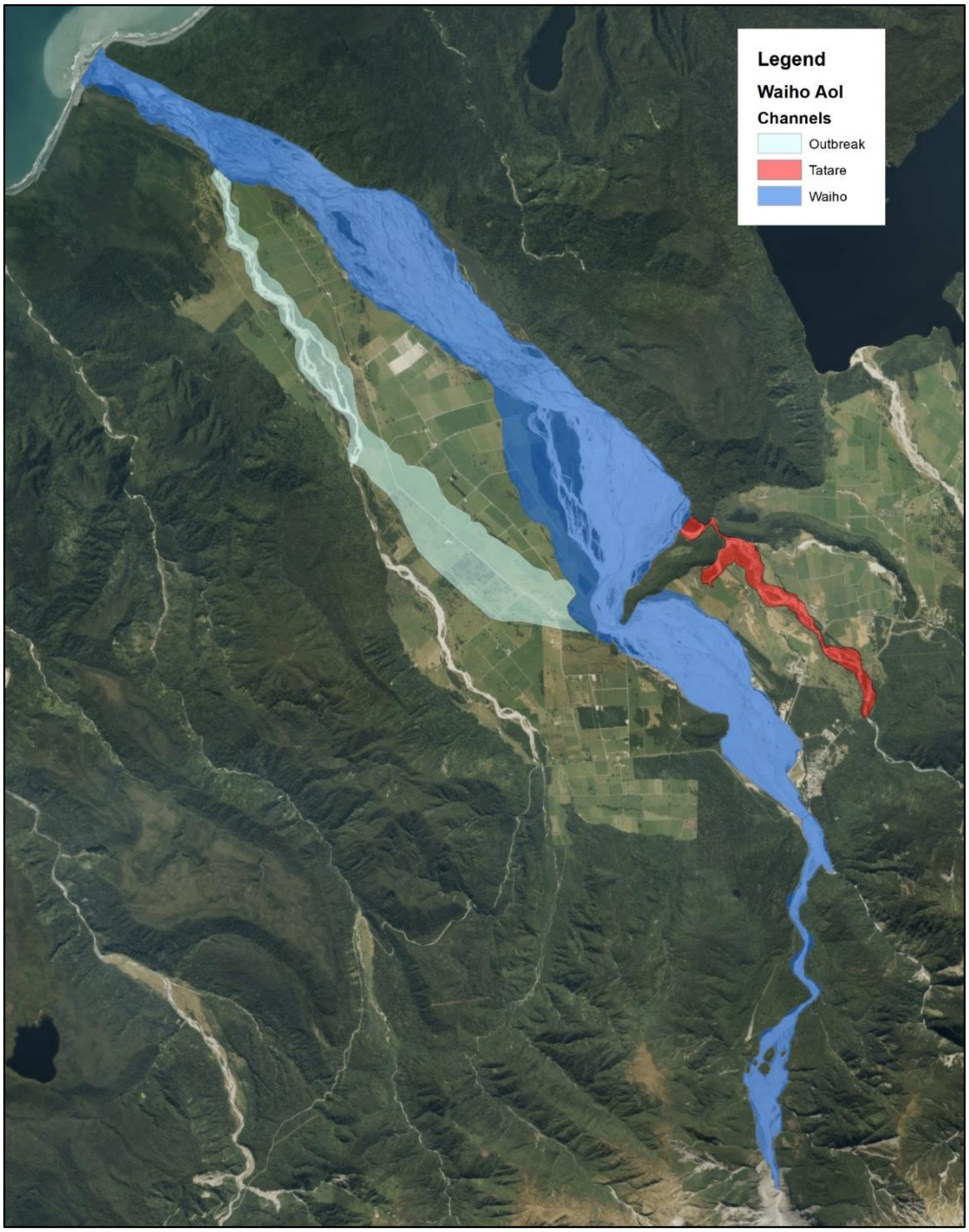

Figure 3-3 – Area of Interest for Change Analysis

3.4 SUB REACH ANALYSIS

In addition to reporting volumetric changes in the three areas identified in the area of interest, analysis of the Waiho River was been split into a series of downstream units or 'cells', in order to quantify the longitudinal pattern of bed response from the glacier to the coast.

Two different models of downstream cells were used. First, the analysis has been divided up into reaches delimited at each end, by the location of historic cross section surveys (XS0-XS23). This approach provides a spatially integrated measure of bed level change between the repeatedly surveyed sections, providing a robust insight into the local pattern of change that averages out the sampling bias due to the siting of specific cross-section.

However, as the historic cross sections do not extend significantly downstream of the Waiho Loop (XS-23), a separate longitudinal analysis has also been completed, in which the entire length of the river was divided into a set of regular 500 m cells based on the channel centreline.

The resulting pattern of sub-areas (cells) for each of these two longitudinal models is shown in Figure 4-1 and Figure 4-2 on the following pages.

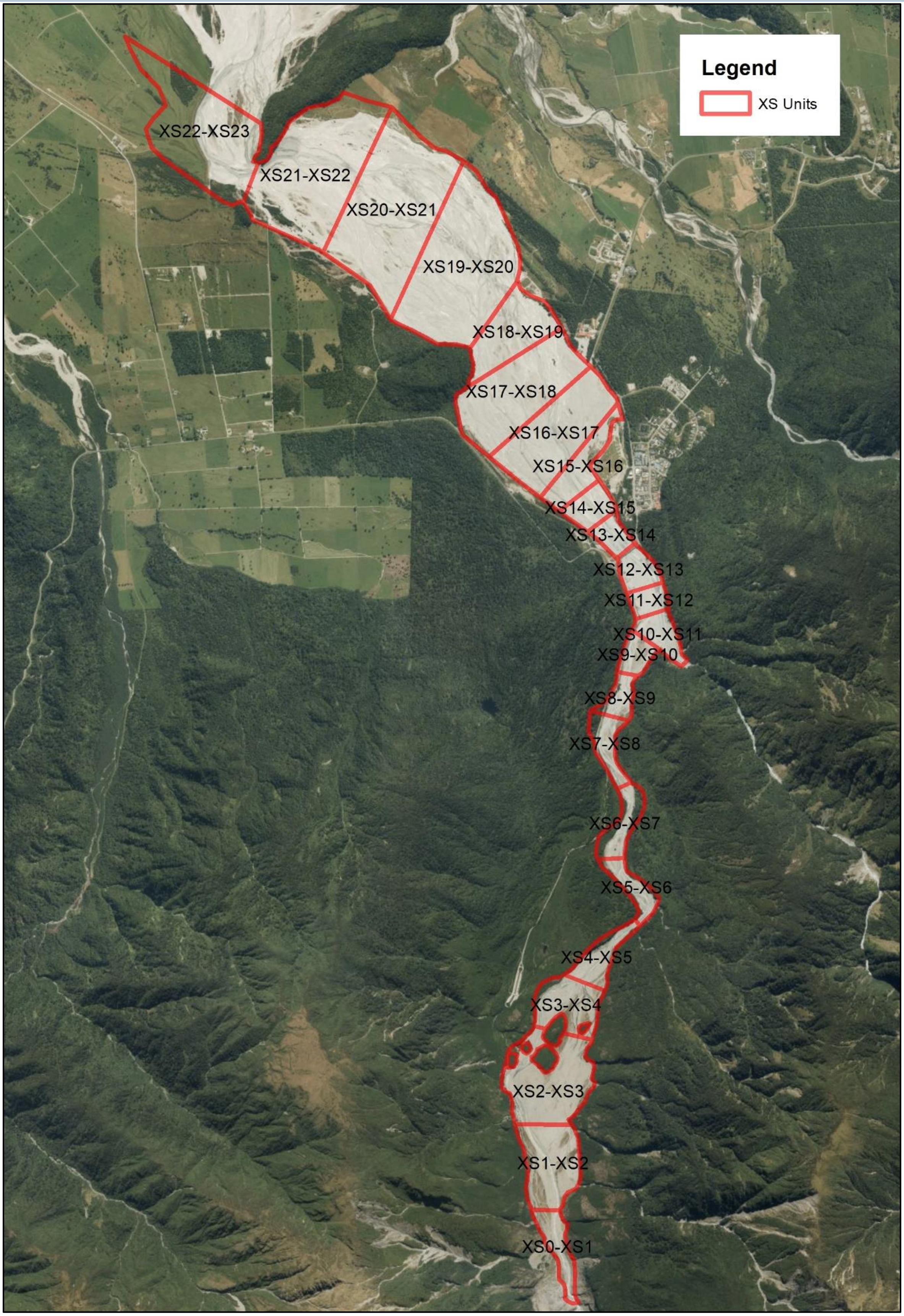

Figure 3-4 – XS Units

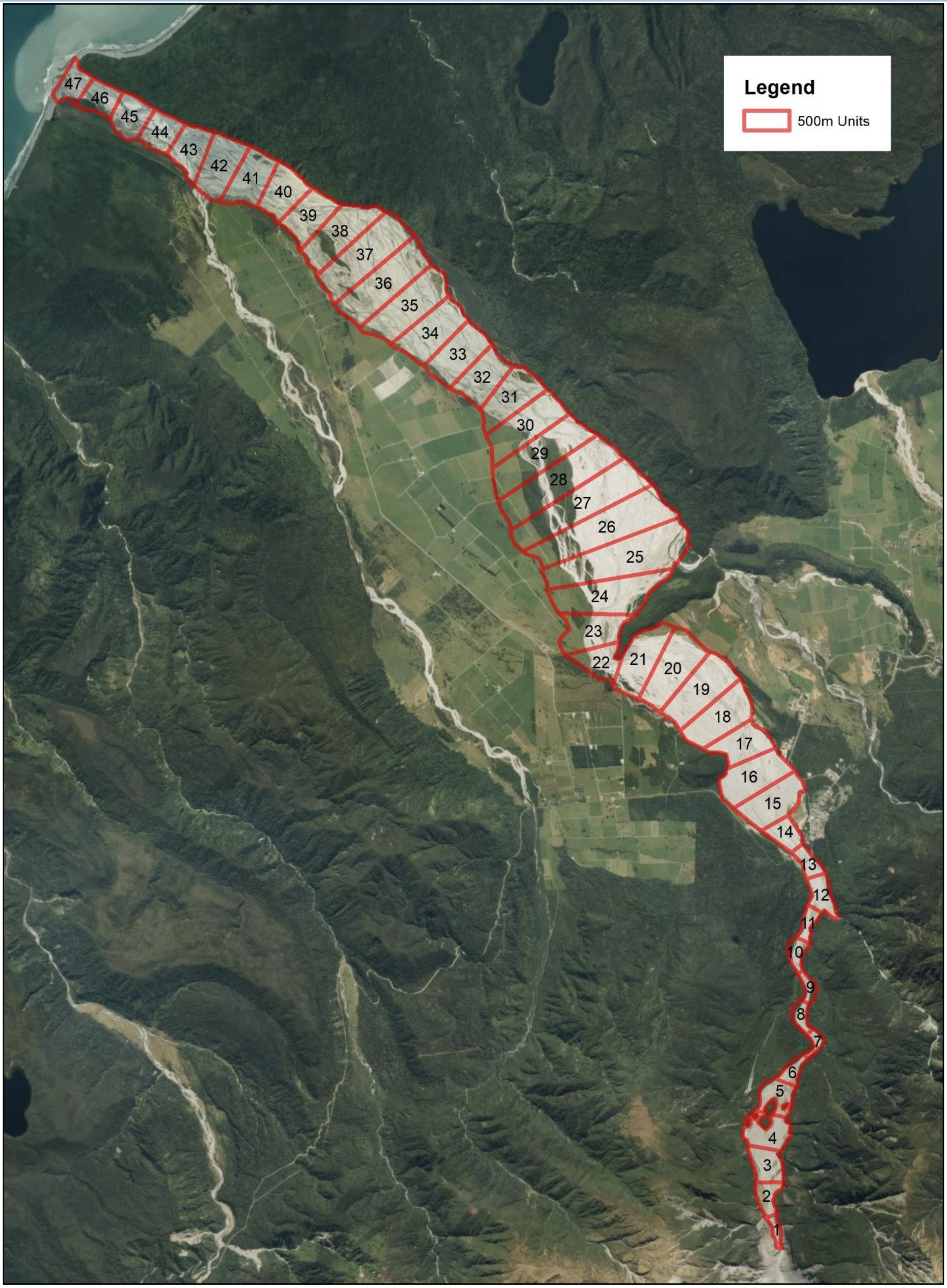

Figure 3-5 – 500m Longitudinal Units

4. RESULTS PRESENTATION

4.1 BROADSCALE PATTERNS OF BED-LEVEL CHANGE AND CHANNEL ADJUSTMENT

4.1.1. VOLUMES OF EROSION AND DEPOSITION

The aggregated volumes of erosion and deposition and the total net difference (net difference = deposition – erosion) for the three main areas of interest are summarized below in

Table 4-1 below. For all three areas, the net difference is positive, indicating an increase in sediment storage (an increase in bed level).

Table 4-1 -Summary of thresholded volume differences within AOI

	Volume Erosion (m^3)	+- Error (m^3)	% Error	Volume Deposition (m^3)	+- Error (m^3)	% Error	Net Volume Difference (m^3)
Waiho	**3,677,044**	876,810	23.85	**6,676,789**	1,535,078	22.99	**2,999,745**
Tatare	**364,640**	57,109	15.66	**372,244**	87,744	23.57	**7,604**
Outbreak	**245,911**	77,876	31.67	**588,866**	226,455	38.46	**342,955**

Along the mainstem of the Waiho, from the Glacier to the mouth, the depositional signal is exceptionally strong, with over 6.6 M m^3 of sedimentation and a net increase in sediment storage of nearly 3 M m^3. When averaged over the 19 km^2 area of interest (shown in blue in Figure 3-3), this represents an average, system wide, increase in bed level of 0.16 m.

In the Tatare Stream, the volumes of erosion and deposition are approximately balanced, with infilling of the historic channel compensated by significantly local widening of the channel (see discussion below).

Volumetric changes along the path of the outbreak flood reveal the expected pattern of significant sedimentation with over 0.58 M m^3 of deposition and a net increase in sediment storage of 0.34 M m^3 within the area of interest. It should be noted, that the changes within this region reflect significant reworking along the lower reaches of Docherty's Creek in addition of sedimentation from the outbreak through Milton's Bank.

4.1.2 VISUAL INTERPRETATION OF CHANNEL CHANGES

A visual representation of the observed pattern of bed level adjustment between the two surveys is shown by the DEMs of Difference (DoDs) presented in Appendix A. To aid visualisation, the results have been split across three maps representing key areas of interest as follows:

- Glacier to Callery Confluence
- Callery Confluence to Waiho Loop (incorporating the Tatare Stream area of interest)
- Waiho Loop to Coast (incorporating the breakout from Milton's Bank).

Due to the significant differences for the range of bed level change for each of the three maps, each map has used a different set of intervals for the colour legend.

GLACIER TO CALLERY CONFLUENCE

This 6 km reach exhibits a major adjustment in both planform and bed level. In the first 2 km immediately downstream of the glacier, the riverbed has aggraded significantly, with sedimentation widely exceeding 5-8 m, infilling the historic incised channel. Figure 4-1 shows a cross-section extracted at a distance of 500 m downstream from the upstream limit of the lidar surveys (at the interface between cells 1 and 2 in Figure 3-5 above). Here, the blue profile represents the river section extracted from the 2016 lidar and the red the resurveyed profile from the 2019 survey. While, some caution must be taken to reflect the lack of a bathymetric correction in 2019, the scale and extent of channel is clearly evident, with over 10 m of channel fill locally and between 5-8 m across the active valley width.

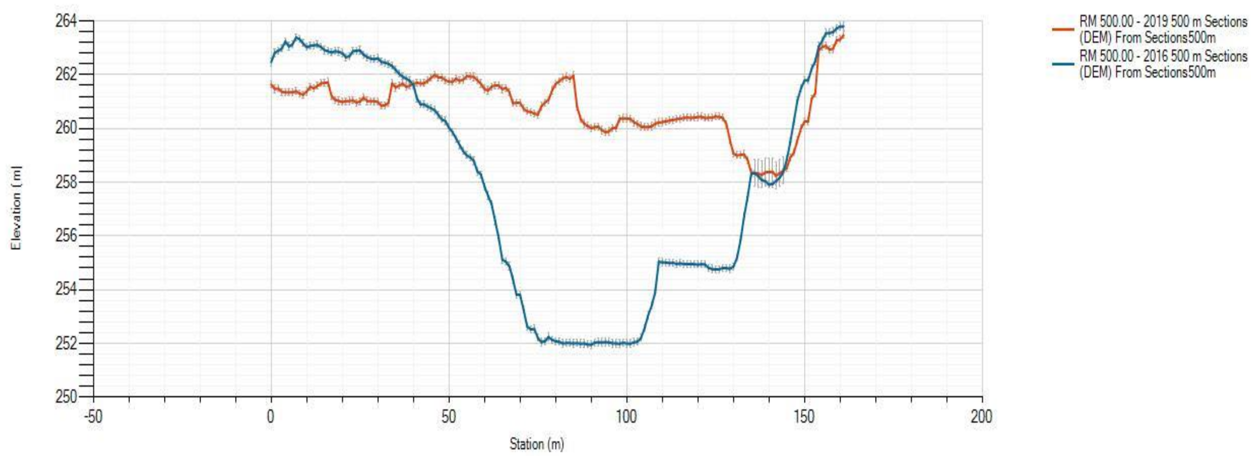

Figure 4-1 Comparison of valley floor profiles extracted from the 2016 and 2019 surveys 500 m downstream from the upper extent of the lidar surveys

Infilling of the 2016 true-left channel continues downstream of Teichelmann and Sentinel Rocks, while flow convergence around these islands has induced scour on the true-right of the active fairway. Between Sentinel Rock and the Callery confluence, channel adjustment comprises infilling of the historic channel and periodic but significant widening of the valley floor associated with erosion on the outer bends of the sinuous channel. Widening of the valley floor exceeds 70 m on the outside bends, resulting in a major influx of material into the channel associated with destabilization of the adjacent slopes which also resulted in a c. 250 m slope failure across the glacier access road around NZTM 1,371,450 E 5,190,400 N.

CALLERY TO WAIHO LOOP

Between the Callery confluence and the SH6 bridge, the river exhibits an approximate balance of erosion (sourced from cliff retreat on the true right) and channel infilling. The net result is only minor change in bed level at the bridge. Downstream of the SH6 bridge, there is net scour for c. 1.5 km, before the braidplain widens downstream of the Heliport and a net pattern of bed level increase is established through to the Waiho Loop. Locally depths of sedimentation are very high given the expansive width of the channel, and may exceed 2-3 m widely, with average bed level changes of 0.3-0.7 m.

TATARE STREAM

The Tatare river is incised into the Waiho fan limiting the potential for significant sedimentation as described on the Waiho above. By contrast, the pattern of channel adjustment here can be summarized as a combination of infilling the 2016 channel accompanied by significant local widening on outer bends. The net result is a sediment budget that is more or less in balance, and where increases in bed level are offset by widening of the fairway.

WAIHO MAINSTEM FROM THE WAIHO LOOP TO THE MOUTH

Downstream of the Waiho Loop the riverbed is net aggradational, with a net increase in sediment storage exceeding 1 M m3, in the lower 13 km of the river. This reach includes the breach of Milton's Bank, seen clearly by the pattern of left-bank erosion that traces the arcuate form where the historic stopbank once stood. Reworking of the braidplain in these lower reaches is extensive indicating major resetting of the anabranch network. There is also significant local scour and widening of the fairway, most notably along the right bank downstream of the airfield (between channel units 29-33 shown in Figure 3-5.

OUTBREAK AND DOCHERTY'S CREEK

The lidar surveys capture the outbreak flood along the true left of the lower Waiho valley, originating from the breach at Milton's Bank. The breakout joins Docherty's Creek at NZTM 1364,900 E 5197250 N. Immediately downstream of the breach, there is significant sedimentation over existing paddocks, Waiho Flat Road and Franz Josef Aerodrome. The pattern of sedimentation observed in the DoD is concentrated in historic palaeochannels, where depths of fill widely exceed 0.4-0.6 m. The extent of overbank sedimentation is likely to be a conservative estimate however, as the uncertainty analysis used in the DEM differencing (based on areas covered by grassland in both surveys) limits the detection of elevation change to a threshold level of 0.32 m. The actual extent of sedimentation is therefore likely to be significantly underestimated.

4.2 CROSS SECTIONAL ANALYSIS

A more detailed analysis of bed level and volume changes along the main Waiho River has been carried out by dividing the river into sub-reaches, using the historical cross section locations as end-points between spatial units (as shown in Figure 3-4). This permits analysis of the average change in bed level between sections and thus reduces the local bias associated with singular measures at specific sections. A summary of the results is presented in Table 4-2 below.

Table 4-2 – Summary of bed level and volume change between cross sections

	Cross Section	Bed Level Change (m)		Volume Change (m^3)	
		DZ	Error		
Glacier to Callery Confluence	XS0-XS1	2.98	± 0.19	277,817	±17,263
	XS1-XS2	2.21	± 0.19	486,570	±41,686
	XS2-XS3	0.81	± 0.17	220,568	±45,631
	XS3-XS4	0.70	± 0.18	95,745	±24,815
	XS4-XS5	0.20	± 0.25	17,723	±22,262
	XS5-XS6	0.78	± 0.23	52,555	±15,568
	XS6-XS7	-1.55	± 0.21	-142,315	±19,654
	XS7-XS8	-1.95	± 0.19	-141,705	±13,926
	XS8-XS9	0.45	± 0.19	23,155	±9,670
	XS9-XS10	0.79	± 0.17	33,633	±7,313
Callery Confluence to end of Helipad Bank	XS10-XS11	-0.08	± 0.25	-4,247	±13,519
	XS11-XS12	-0.94	± 0.18	-35,746	±6,791
	XS12-XS13	0.55	± 0.18	25,528	±8,433
	XS13-XS14	-0.06	± 0.17	-2,557	±7,316
	XS14-XS15	-0.35	± 0.18	-24,718	±12,856
End of Helipad Bank to Waiho Loop	XS15-XS16	-0.02	± 0.15	-2,278	±14,142
	XS16-XS17	0.05	± 0.14	14,718	±42,110
	XS17-XS18	0.42	± 0.15	134,797	±47,797
	XS18-XS19	0.70	± 0.16	131,761	±29,644
	XS19-XS20	0.32	± 0.15	162,480	±77,470
	XS20-XS21	0.47	± 0.16	251,304	±82,739
	XS21-XS22	0.65	± 0.19	289,959	±83,278
	XS22-XS23	0.26	± 0.17	86,523	±55,908

The longitudinal pattern of erosion and deposition, as well as a cumulative total volume change based on these units is also presented below in Figure 4-1. This analysis quantifies the downstream patterns of channel adjustment mapped in the Appendix and described in Section 4.1. Units XS0-XS04 demarcate the extensive fill at the head of the Waiho valley, comprising a net increase in sediment storage of more than 1 M m^3 of sediment. The erosional input into the system between XS06-XS08 reflects the extensive channel widening and associated toe-slope failures through the confined reach before the Callery confluence. The bed level change between XS08-XS16 is then predominantly degradational before extensive sedimentation occurs as the river widens towards the Waiho Loop (XS16-XS22).

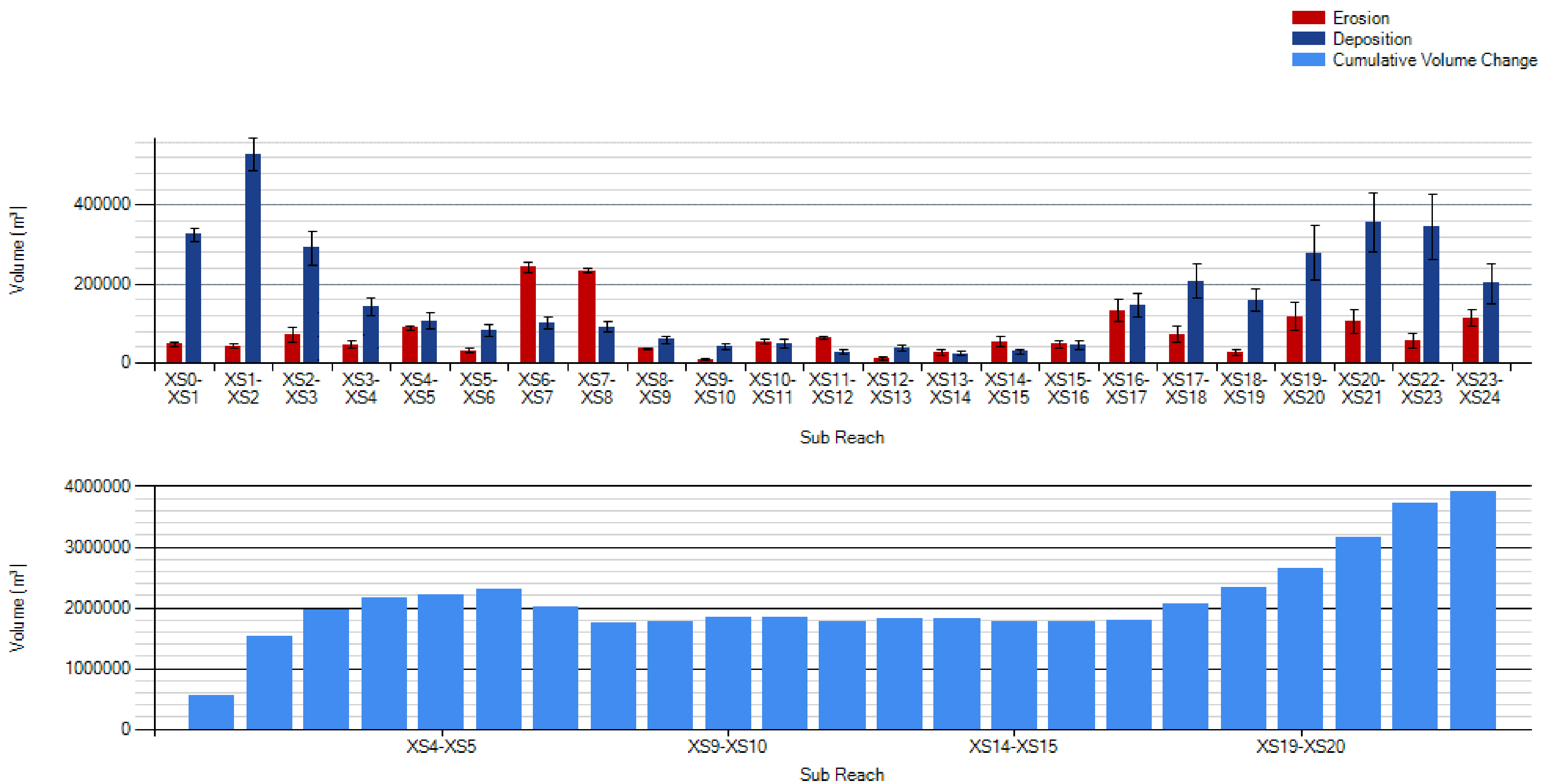

Figure 4-1 – Summary of erosion and deposition and cumulative volume change between XS 1 to XS23

4.3 LONGITUDINAL ANALYSIS BASED ON 500M UNITS

A longitudinal analysis of volume changes was also undertaken along the entire length of the Waiho River, dividing the river into 500 m units starting at the glacier and working downstream. In total the river is divided into 47 longitudinal units, representing the full 23.5 km centreline length. A summary of the erosion and deposition changes for each of these units as well as a cumulative total volume change are plotted in Figure 4-2 below.

This sequence reveals the dominant aggradational pattern, from source to sink. The net volumetric change of +3.3 M m^3 represents the minimum coarse sediment yield from the combined Waiho and Callery catchments over c. 3-year period between the surveys. Given the high frequency of floods through the system, it is impossible to attribute all of this material to the single event at the end of March 2019, but it seems likely that this will represent the dominant driver of the observed pattern.

The downstream series plotted in Figure 4-2 shows three major areas of sedimentation: a) in first 1-3 km immediately downstream of the glacier (units 1-5); b) river distances 8-11 km, upstream of the Waiho Loop (units 16-21); and c) at river distance 12.5-14 km, on the distal margins of the fan downstream from the Waiho Loop (units 25-28). Areas dominated by erosional signal are limited to the areas of valley widening just upstream of the Callery confluence (river distances 4-5 km, units 9-10) and to a lesser degree, downstream of the SH6 bridge between units 12-14.

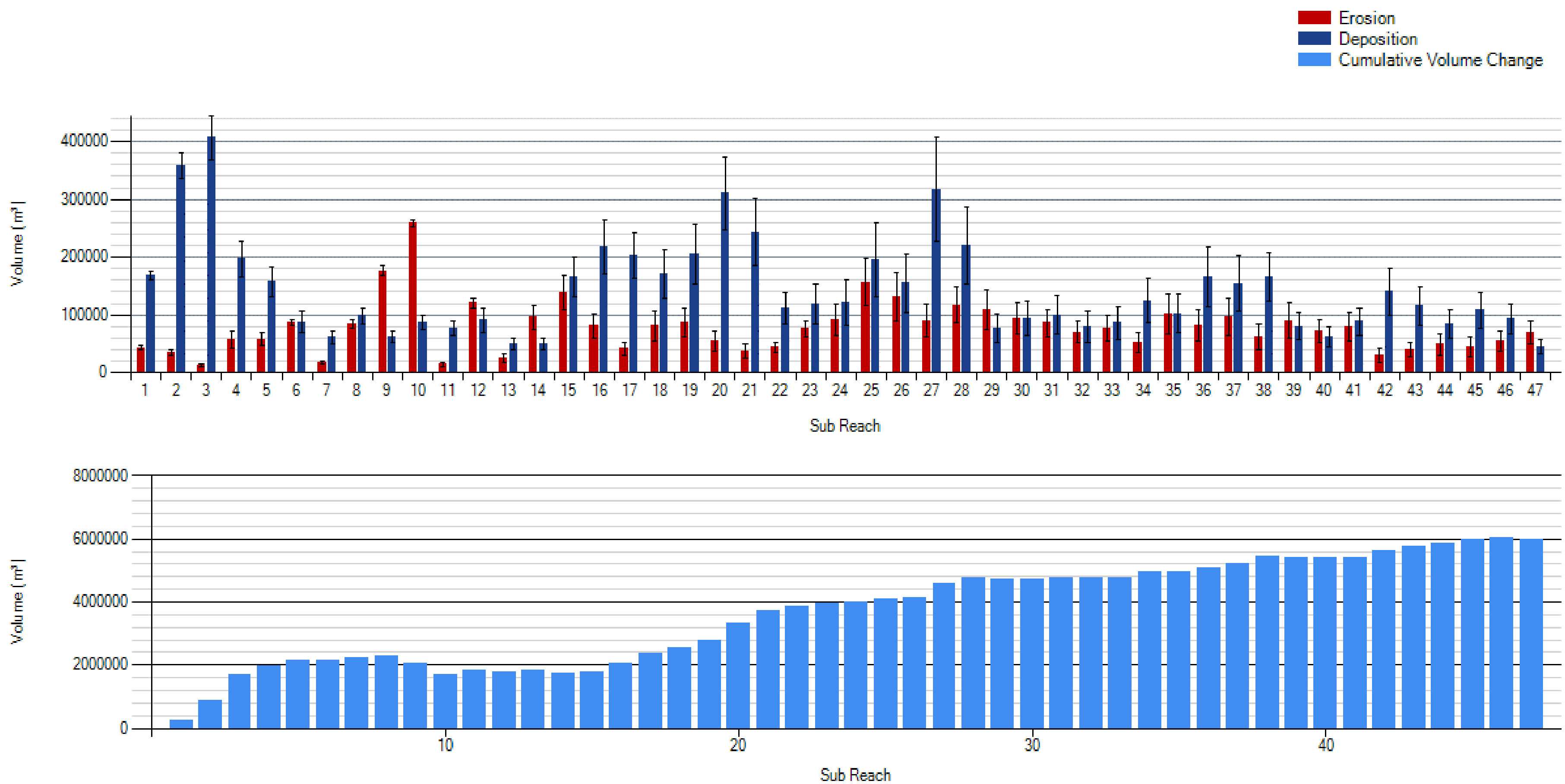

Figure 4-2 - Summary of erosion and deposition and cumulative volume change for whole reach based on 500m units

5. CROSS SECTION MEAN BED LEVEL ANALYSIS

In order to allow a comparison with historic cross-sectional survey data on file, a basic mean bed level analysis has also been carried out at each of the historic cross section survey locations.

Unlike the 2-dimensional analysis carried out using the LiDAR with the GCD tools, no adjustment has been made with the 2019 dataset in order to account for the water surface for the cross sectional analysis, so the results have a greater degree of uncertainty and will slightly overestimate the overall mean bed level for the 2019 survey. However, considering the water surface only covers a small area of the active channel, the overall conclusions and trends are considered valid.

A summary of the changes in mean bed level from 1983 to 2019 is presented in Table 5-1 on the following page with plots showing the cumulative change from 1983 for each surveyed cross section presented in Appendix B.

The overall trends match fairly closely with the results of the GCD analysis presented in section 4, however some cross sections are showing localised increases (such as at XS6 and XS7) whereas the GCD analysis between sections 6 and 7 shows a significant decrease in MBL and volume. Inspection of the LiDAR shows that this decrease in mean bed level between the cross sections is due to significant lateral erosion as was alluded to in section 4-2. Figure 5-1 presents this clearly by showing a comparison of the 2017 and 2019 imagery and results of the GCD analysis. The dark red areas on the GCD plans highlight significant lateral erosion in these outer bends.

Table 5-1 – Summary of Mean Bed Level based at historic cross section locations

	Mean Bed Level (m)												MBL Change (m)	MBL Change (m)
	1983	1990	1993	1999	2002	2008	2011	2012	2014	2015	2016	2019	1993 to 2019	2016 to 2019
CS1			245.5	253.0		253.1				250.7	250.6	253.8	8.2	3.2
CS2	226.0	229.4	229.5	234.5		234.0				233.3	233.6	235.1	5.5	1.5
CS3	212.8	214.0	214.6	216.3		216.4				217.2	217.3	217.6	3.0	0.3
CS4	205.2		206.8	207.8		207.6				207.8	207.5	208.6	1.8	1.1
CS5	195.8	196.1	196.0	195.9	195.9	195.7				196.0	196.3	198.4	2.4	2.2
CS6	185.4	185.3	184.9	185.3	185.3	184.7				185.4	185.0	186.8	1.9	1.8
CS7	173.5	172.5	173.3	175.0	175.0	175.5				174.9	175.0	176.2	2.9	1.2
CS8	163.6	163.5	164.8	166.4	166.4	167.2				167.0	167.3	168.2	3.4	0.9
CS9	157.4	157.2	159.2	161.7	162.1	162.0				162.3	162.5	163.8	4.5	1.2
CS10	152.8		154.2	158.0	158.0	158.3	160.2	160.1	159.5	159.4	159.4	159.6	5.4	0.3
CS11	149.9	151.4	152.5	155.0	154.8	155.7	157.8	157.3	156.7	156.3	156.8	157.2	4.7	0.4
CS12			150.0	152.6	153.1	153.3	155.0	154.4	154.4	154.2	154.2	154.9	4.9	0.7
CS13	145.7	145.1	145.9	148.9	148.4	149.1	150.6	150.0	150.5	149.9	150.5	150.5	4.6	0.0
CS14			143.6	146.3	145.9	146.6	147.6	146.8	147.8	147.7	148.0	147.6	4.0	-0.4
CS15			141.2	143.2	143.4	143.7	144.5	144.5	144.9	144.6	145.1	144.7	3.5	-0.3
CS16			137.7	139.2	139.6	139.8	140.2	140.2	140.5	140.5	140.9	140.9	3.2	0.0
CS17			133.1	134.3	134.4	134.6	135.2	135.2	135.6	135.7	136.0	136.2	3.1	0.2
CS18			127.8	128.7	128.9	129.2	129.7	129.7	129.8	129.8	130.1	130.7	2.9	0.6
CS19	123.6		124.0	124.3	124.6	124.8	125.2	125.3	125.2	125.3	125.6	126.5	2.5	0.9
CS20	116.9		117.1	117.4	117.4	117.9	118.3	118.4	118.5	118.8	118.7	119.1	1.9	0.4
CS21	109.1		109.1	109.2	109.2	109.4	109.5	109.6	109.6	109.7	109.7	109.9	0.9	0.2
CS22	101.4		100.9	101.0	101.0	101.0	101.0	100.8	100.9	101.0	100.9	101.7	0.8	0.7
CS23	93.4		94.5	94.5	94.7	95.0	95.0	94.9	95.0	95.1	95.1	95.7	1.2	0.6

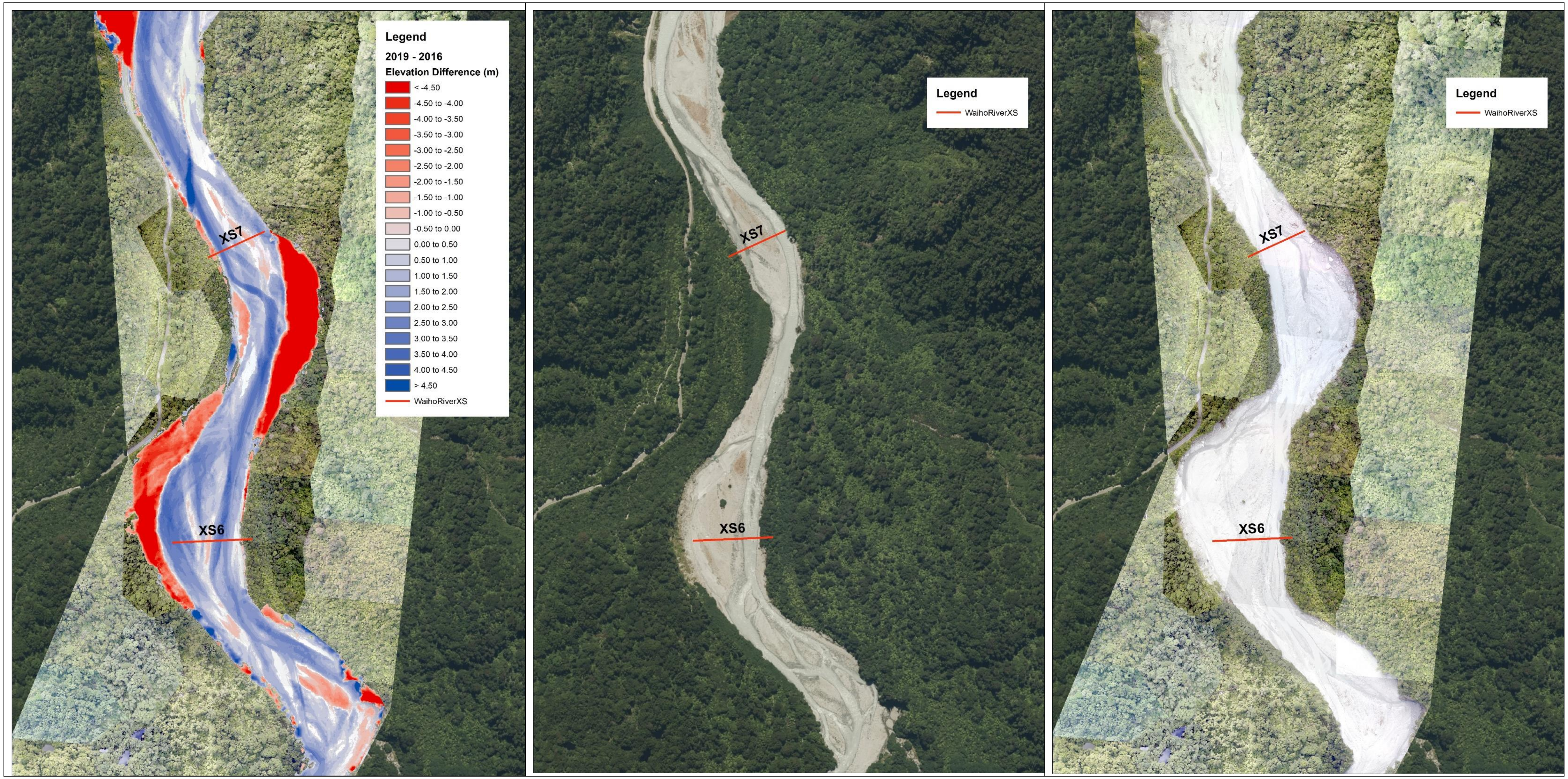

Figure 5-1 – Change in elevation at XS6 at XS7 between 2016 and 2019 LiDAR (left), 2017 aerial imagery (centre), 2019 aerial imagery (right)

In general the following conclusions can be drawn from the cross sectional mean bed level (MBL) analysis (see Appendix B for cumulative plots of MBL change).

XS1 to XS2 – the trends of degradation which had been observed from 2008 to 2016 have now been reversed with very significant aggradation present at these two sections. MBL are now higher than they were in 2008.

XS3 to XS4 – these two cross sections appear to have continued the historic rate (and apparently consistent) aggradation since 2016.

XS5 to XS6 – these two cross sections have been consistently stable since 1983. Bed levels at both of these cross sections has sharply increased for the first time since 1983, with the MBL increasing by over 2m at XS5.

XS6 to XS9 – these three cross sections have all increased in MBL at a greater rate than in the previous 15 years. The rate of aggradation since 2014 appear to be similar to the rate observed between 1990 and 1999

XS10 to XS16 – this reach has been historically aggrading, however appears to be behaving as a transfer reach (ie sediment is passing through this reach rather than being stored). MBL have had little change in this reach.

XS17 to XS21 – this reach appears to be aggrading at a slightly accelerated rate in comparison to the years from 1983 to 2016. Due to the very wide width of the river here, the volume of sediment accumulation is very significant. This indicates that the material that was previously aggrading in the reach between the Callery River and the Heliport bank is now being transferred through to this area and is aggrading here rather than upstream. If this rate of aggradation continues then significant pressure can be expected on the bank protecting the treatment ponds on the true right bank.

XS22 to XS23 – Both of these sections have increased significantly in the last three-year period. This is the first time that section 22 has had a significant increase since 1983. This may indicate that the gravel fan is beginning to extend beyond the Waiho Loop.

6. DISCUSSIONS

6.1 IMPACT OF WEATHER PATTERNS ON SEDIMENTATION

It is very difficult to predict with any certainty future behaviour of such a complex natural system, however historic trends can give some insight as to what may occur in the future.

The main Alpine Fault crosses the Waiho River, dividing the mountainous upper catchment from the coastal plains. This fault line is known to rupture on a regular basis giving rise to significant inputs of fractured rock into the river systems. Due to the mid-latitude location in the southern Pacific Ocean, with the Alps intercepting the westerly circulation of anticyclones and depressions, the area is also prone to very high rainfall intensities (Gardner & Williams, 2019)

Flood flows are generated rapidly through the catchment and the steep nature of the Waiho River gives rise to very high rates of sediment transport over short time periods. The high relief in the vicinity of the river also comprises weak, fractured rock which results in very high rates of sediment supply even under the natural forest cover.

The oceanic climate is highly variable but subject to long-term oscillations of large global circulations, specifically the Southern Ocean circulation and circulations around the South Pacific (Gardner & Williams, 2019). The Interdecadal Pacific Oscillation (IPO) is a major driver of regional variations in storm intensity and flood flows in New Zealand. This has a typical cycle with 20-30 year phases (positive & negative) which gives rise to periods of high flood intensity followed by a generally quiescent period, before a return to more and larger floods.

For the Waiho River of the Franz Josef Glacier system, there is some evidence of a correlation between glacier advance and rising mean bed levels at the State Highway (SH) Bridge. Conventionally, this association is interpreted to reflect increased sediment supply associated with high rates of glacial erosion during periods of advance. An alternative explanation, however, is that the bed level response actually reflects increased erosion due to elevated rainfall, which in turn leads to a positive glacier mass balance and so also causes glacier advance (albeit with the terminal response lagging). Such behaviour would be expected during the positive phase of the IPO and provides an alternative causality for the correlation of glacier advance and bed level change.

Analysis of the hydrological records of several West Coast rivers (Whataroa, Grey and Buller) indicates that the regional climate seems to have been in the negative phase of the IPO cycle since the late 1990's. The negative phase of the cycle correlates to generally lower overall rainfall intensities, indicating that the last 20 years or so has been a relatively quiescent period for the West Coast. Increased rainfall events as of late may be indicating that the cycle has changed to a positive phase suggesting we can expect more increased rainfall events for the next 20 to 30 years. Increased rainfall intensities will ultimately lead to an increase in sediment supply into the West Coast rivers and will likely lead to a change in sedimentation patterns.

Increased rainfall volumes in the Waiho River catchment will be very likely to mobilise the sediment, which is currently stored in the upper Waiho River, as well as mobilise greater volumes of the fractured material present in the steep valley slopes, leading to even greater volumes of sediment in the river. It is likely that this material will continue to deposit downstream of the SH Bridge, however there is also significant likelihood based on past behaviour that the reach between the Callery confluence and the Helipad bank may return to being in an aggradational phase, although this will also be influenced by the volume of material coming into the system from the Callery River system.

One thing to keep in mind is that the climate is changing fairly rapidly and this appears to be impacting on the behaviour of the global climate patterns. As a result, historic behaviour may no longer be as good an indicator as to what will happen in the future. Recent events such as tropical cyclone Gita and Fehi coming as far south as the top of the South Island do not fit normal patterns of weather behaviour for New Zealand and indicate that global weather patterns are changing as the seas warm etc. These changes in weather patterns may be a further indicator that the West Coast may be in line for even greater storm intensities in coming decades, which will likely lead to even greater volumes of sedimentation in the West Coast rivers, including the Waiho River.

6.2 FUTURE SEDIMENTATION TRENDS

As has been highlighted above, it is likely that increased volumes of sediment will continue to enter the Waiho River. We consider the following trends to be likely;

- The fan will continue to build downstream of the Helipad bank. This may lead to increased pressures on the true right embankment protecting the oxidation ponds. Whilst the overall trend is one of aggradation, the rock lined embankment on the true right bank will likely encourage the main braid of the river to flow along the edge of the bank causing significant scour at the toe of the bank. If the stopbank does not have a well-founded toe that extends several metres beneath the current bed, there will be a reasonable risk of failure of this bank, no matter how thick it is.
- Based on historic behaviour there is a chance that the reach between the helipad bank and the confluence of the Callery River will return to an aggradational condition due to the increased volume of sediment now stored in the upper reaches of the river. Historically, there has been a delay between upstream storage and downstream increase in MBL at the SH bridge which is an order of a decade. While a similar lag-time could be likely, the precise link between upstream storage and downstream bed level change will dependent on the frequency of flood events with sufficient energy to transport the material downstream.
- It is likely that the fan will continue to grow and increase bed levels downstream of the Waiho Loop, potentially increasing the pressure on Milton's bank, which was destroyed in the March 2019 flood event and has now been rebuilt.
- While the increase in sediment storage in the main Waiho River system is estimated to be in excess of 3 M m^3, it is helpful to put this in context. For example, in the Fox River catchment (South of the Waiho River) debris flows in the Alpine Gardens and Mills Creek area have fed greater than twice this volume of debris into the Fox River between March 2017 and June 2018. Volume estimates indicate that the volume of debris entering the river system is in excess of 6.5 M m3 (Massey, et al., 2019). Due to the similar nature of the bedrock and relief in the Waiho and Callery River catchments, it would not be unrealistic to expect future slips of a similar magnitude in this catchment. Such events would lead to very significant bed level changes in the river.

- When the Alpine Fault ruptures (which is very considered likely in the coming decades), the system will be essentially reset due to exceptionally large volumes of sediment supply that will result in dramatic changes in river morphology and behaviour.

7. CONCLUSIONS

The following conclusions can be drawn from this analysis.

- Significant volumes of sediment have entered the Waiho River system since the last LiDAR survey was carried out in 2016. It is likely that the rainfall event in March 2019 was the principal driver of this sediment supply.
- A detailed analysis of volume changes has estimated that greater than 3.3 million cubic metres has been deposited in the study area since 2016. This volume represents the minimum plausible rate of catchment sediment supply to the Waiho River, but it is likely that a significant volume of material, in particular finer sediments passed directly through the system to the sea.
- Significant volumes of material have been deposited in the upper reaches of the Waiho River with greater than 1 M m^3 depositing between XS0 and XS5 since 2016. This is a very large volume of material which will ultimately work its way through the system.
- No information on sediment volumes is currently collected in the Callery River catchment which makes up a significant proportion of the overall catchment. Significant volumes of material may have also been destabilised in the March rainfall event which will also eventually make their way into the Waiho River system.
- Based on historic behaviour, significant increases in bed level in the upper Waiho catchment appear to correlate with delayed increases in bed level at the bridge location. There is a chance that the increased bed levels observed in the upper reaches may cause bed levels to aggrade near the bridge in the coming decade. The precise phasing of this connection will depend strongly on the frequency of future storm events.
- A change in weather patterns in the West Coast is likely leading to increased rainfall intensities and as a result increased sedimentation.
- Increased aggradation on the fan downstream of the helipad bank is likely to continue and may lead to increased pressure on the existing stopbanks, in particular the true right stopbank which is protecting the oxidation ponds. If this bank is not well founded with a buried toe, then it maybe at risk of failure in the future due to the fact that it is currently sucking the main braid into the bank.
- Cross sectional analysis shows bed levels aggrading rapidly in the vicinity of the Waiho loop for the first time since the 1980's. This indicates the fan is extending downstream and as the fan continues to aggrade and extend downstream in the vicinity of the Waiho Loop the pressure on the Milton's stopbank may increase as a result.
- With the level of increased aggradation being observed on the Waiho Fan, it is becoming more likely that a permanent avulsion into the Tartare will take place in the future.

8. REFERENCES

Brasington, J., Langham, J. and Rumsby, B., 2003. Methodological sensitivity of morphometric estimates of coarse fluvial sediment transport. *Geomorphology*, *53*, 299-316.

Gardner, M. & Williams, G., 2019. *FOX GLACIER — ROAD ACCESS, ENGINEERING REVIEW,* Christchurch: Land River Sea Consulting Ltd.

Massey, C. et al., 2019. *Landslide hazard and risk assessment for the Fox and Franz Josef Glacier valleys,* s.l.: GNS Science.

Wheaton, J.M., Brasington, J., Darby, S.E. and Sear, D.A., 2010. Accounting for uncertainty in DEMs from repeat topographic surveys: improved sediment budgets. *Earth surface processes and Landforms, 35*, 136-156.

Vericat, D., Wheaton, J.M. and Brasington, J., 2017. Revisiting the morphological approach: opportunities and challenges with repeat high-resolution topography. *Gravel-Bed Rivers: Process and Disasters*, *121*.

APPENDIX A – GCD VISUAL REPRESENTATION

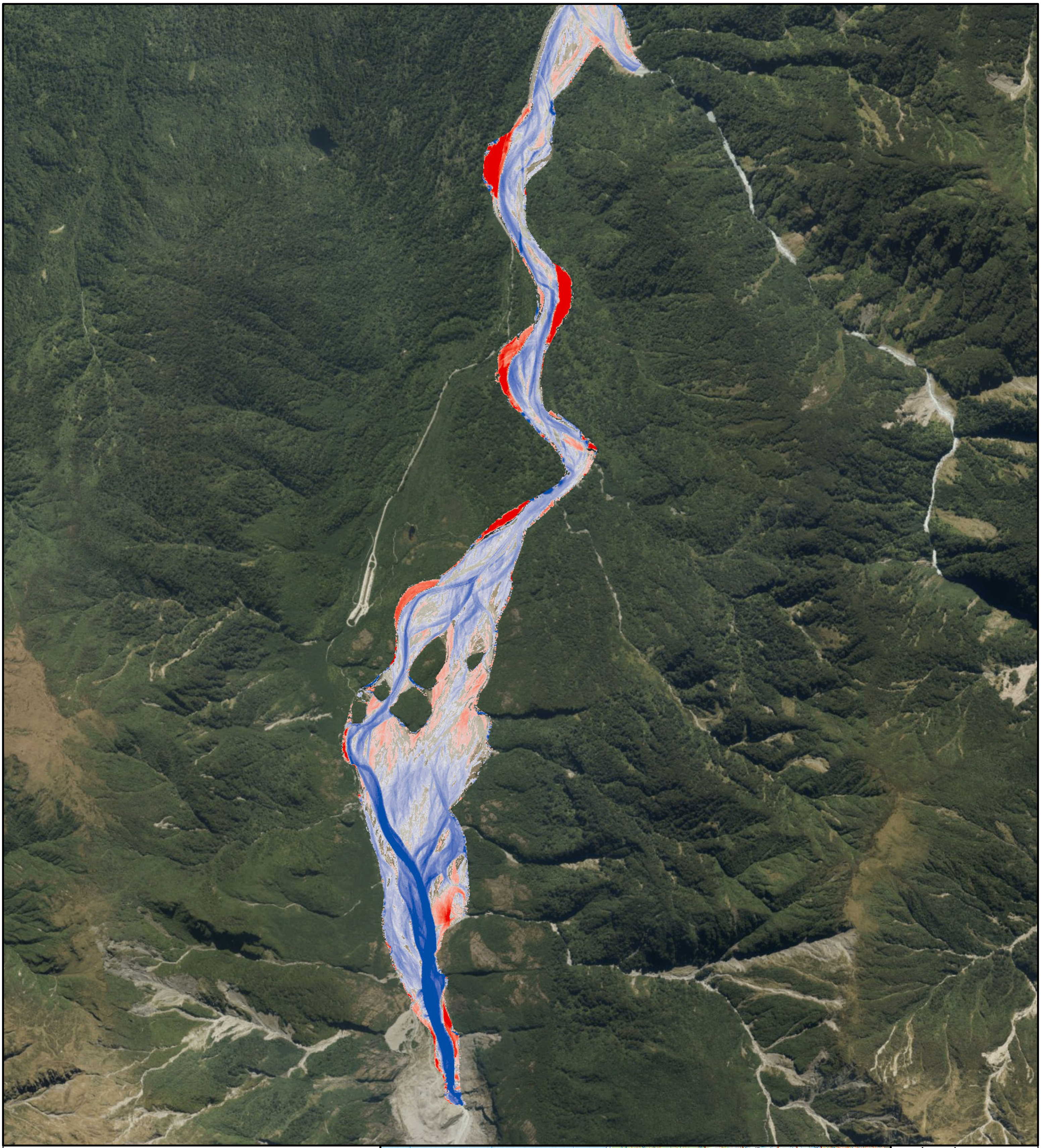

SCALE BAR

0 0.25 0.5 1 km

Legend

2019-2016

Elevation Difference (m)

- < -4.50
- -4.50 to -4.00
- -4.00 to -3.50
- -3.50 to -3.00
- -3.00 to -2.50
- -2.50 to -2.00
- -2.00 to -1.50
- -1.50 to -1.00
- -1.00 to -0.50
- -0.50 to 0.00
- 0.00 to 0.50
- 0.50 to 1.00
- 1.00 to 1.50
- 1.50 to 2.00
- 2.00 to 2.50
- 2.50 to 3.00
- 3.00 to 3.50
- 3.50 to 4.00
- 4.00 to 4.50
- > 4.50

PROJECT

Waiho River Change Detection Analysis

TITLE

Bed Level Change Detection
Glacier to Callery Confluence
Change in bed level 2016 to 2019

LANDRIVERSEA CONSULTING

www.landriversea.com

THE UNIVERSITY OF WAIKATO
Te Whare Wānanga o Waikato

AUTHOR	DATE	JOB CODE	REVISION
Matthew Gardner	29 July 2019	WCRC017	01

N

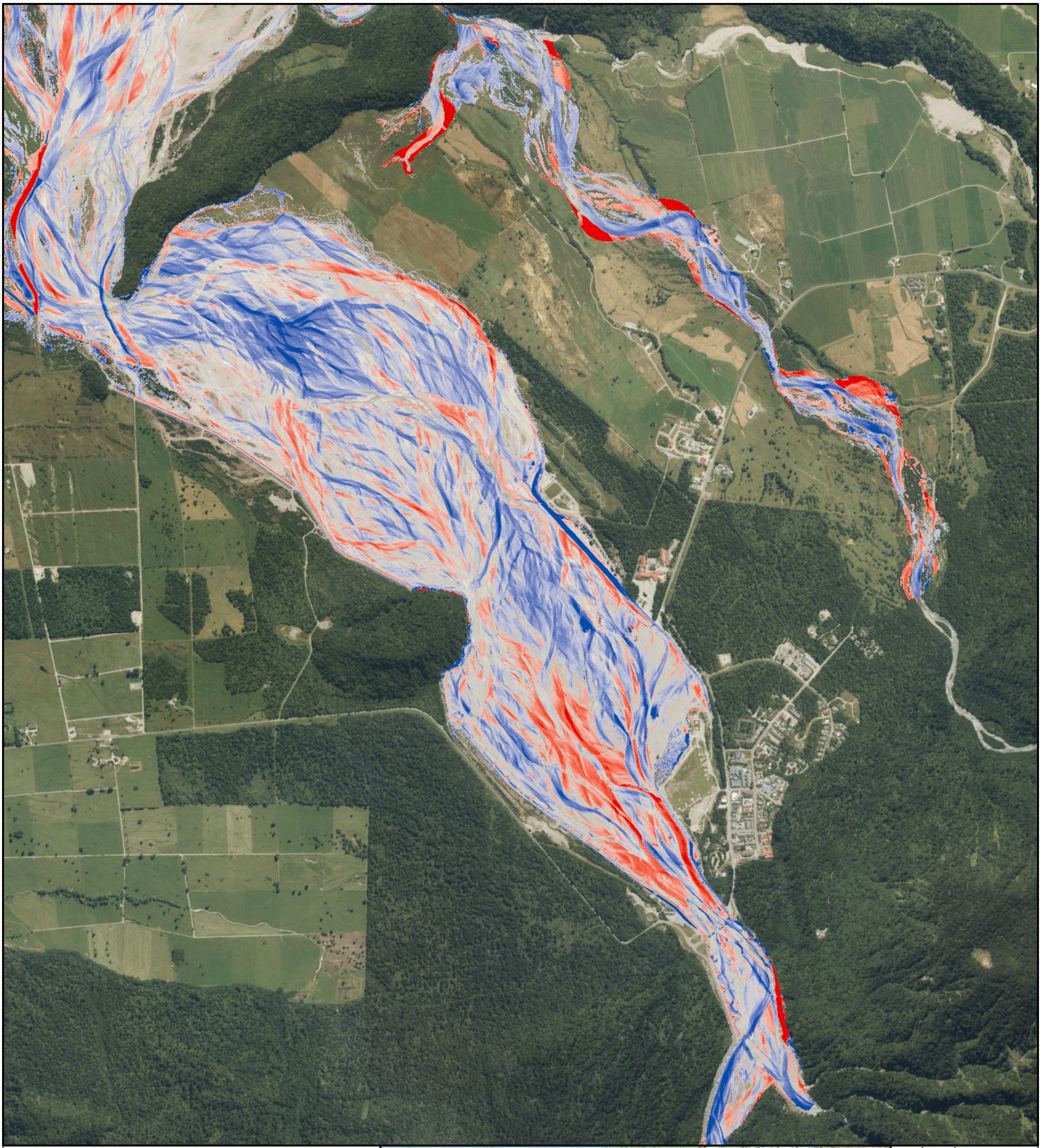

SCALE BAR

0 0.25 0.5 1 km

Legend

2019-2016

Elevation Difference (m)

- < -2.20
- -2.20 to -2.00
- -2.00 to -1.80
- -1.80 to -1.60
- -1.50 to -1.20
- -1.20 to -1.00
- -1.00 to -0.80
- -0.80 to -0.60
- -0.50 to -0.20
- -0.20 to 0.00
- 0.00 to 0.20
- 0.20 to 0.40
- 0.50 to 0.80
- 0.80 to 1.00
- 1.00 to 1.20
- 1.20 to 1.40
- 1.50 to 1.80
- 1.80 to 2.00
- 2.00 to 2.20
- > 2.20

PROJECT
Waiho River Change Detection Analysis

TITLE
Bed Level Change Detection Callery Confluence to Waiho Loop Change in bed level 2016 to 2019

LANDRIVERSEA CONSULTING
www.landriversea.com

THE UNIVERSITY OF WAIKATO
Te Whare Wānanga o Waikato

AUTHOR	DATE	JOB CODE	REVISION	N
Matthew Gardner	29 July 2019	WCRC017	01	

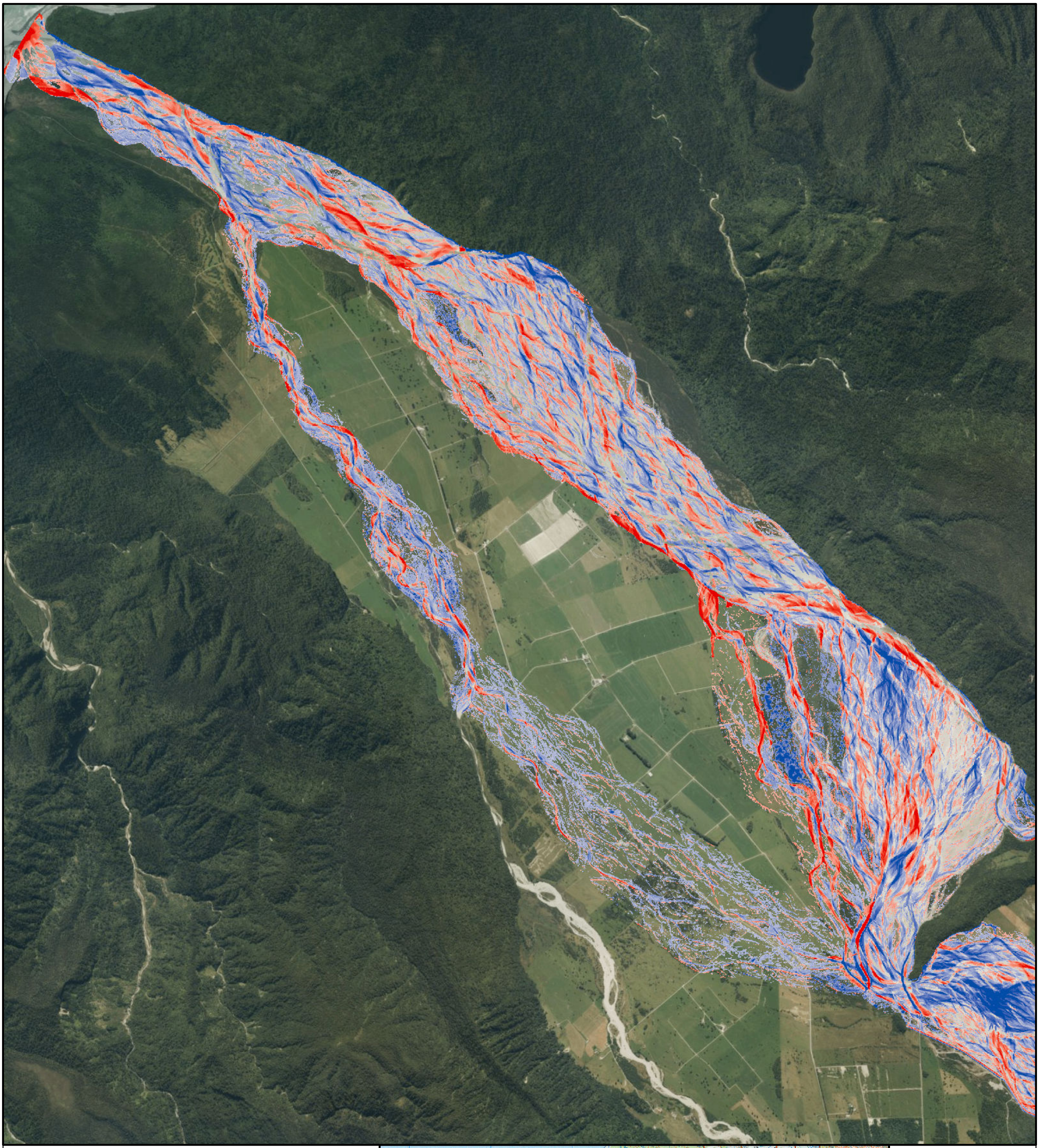

SCALE BAR

0 0.5 1 2 km

PROJECT

Waiho River
Change Detection Analysis

TITLE **Bed Level Change Detection**
Waiho Loop to Mouth
Change in bed level 2016 to 2019

LANDRIVERSEA CONSULTING
www.landriversea.com

THE UNIVERSITY OF WAIKATO
Te Whare Wānanga o Waikato

AUTHOR	DATE	JOB CODE	REVISION	
Matthew Gardner	29 July 2019	WCRC017	01	N

Legend

2019-2016

Elevation Difference (m)

- < -1.40
- -1.40 to -1.20
- -1.20 to -1.00
- -1.00 to -0.80
- -0.90 to -0.80
- -0.80 to -0.60
- -0.60 to -0.40
- -0.40 to -0.20
- -0.30 to -0.20
- -0.20 to -0.10
- 0.00 to 0.20
- 0.10 to 0.20
- 0.30 to 0.40
- 0.40 to 0.60
- 0.60 to 0.80
- 0.80 to 1.00
- 0.90 to 1.00
- 1.00 to 1.20
- 1.20 to 1.30
- > 1.40

APPENDIX B – CROSS SECTIONAL MBL COMPARISON 1983 TO 2019

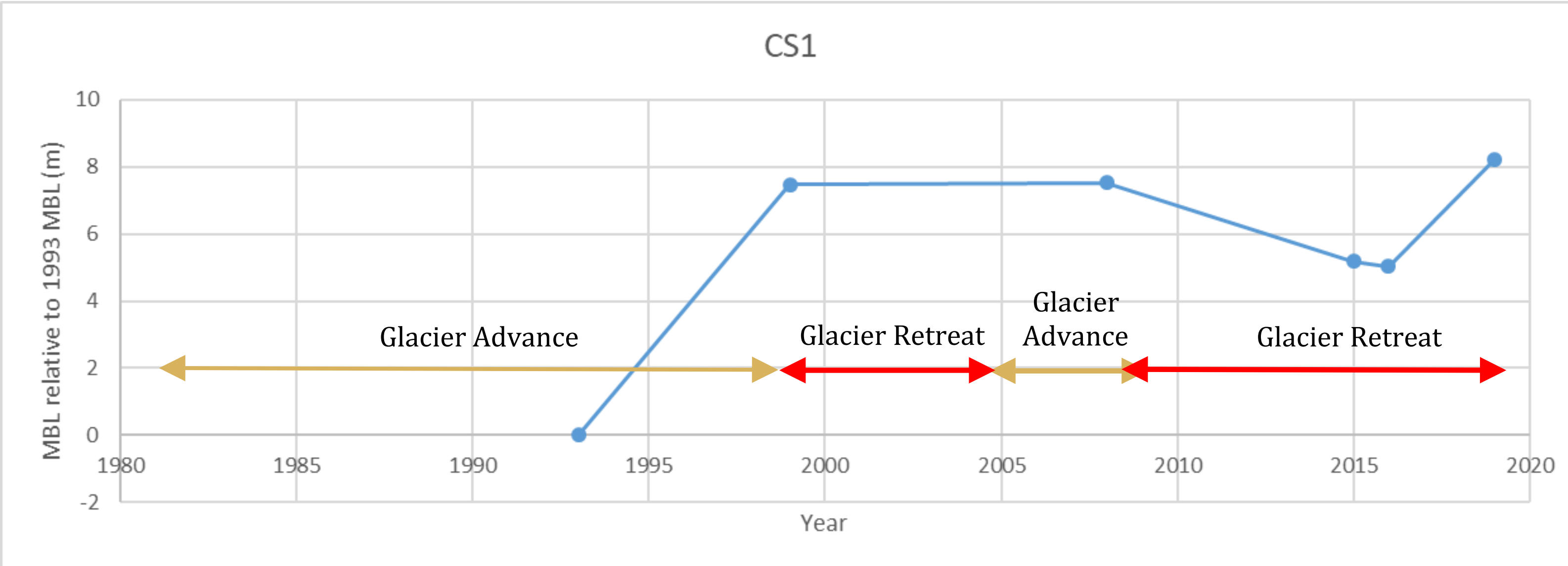
CS1
10
8
6
4
2
0
-2
MBL relative to 1993 MBL (m)
1980
1985
1990
1995
2000
2005
2010
2015
2020
Year
Glacier Advance
Glacier Retreat
Glacier Advance
Glacier Retreat

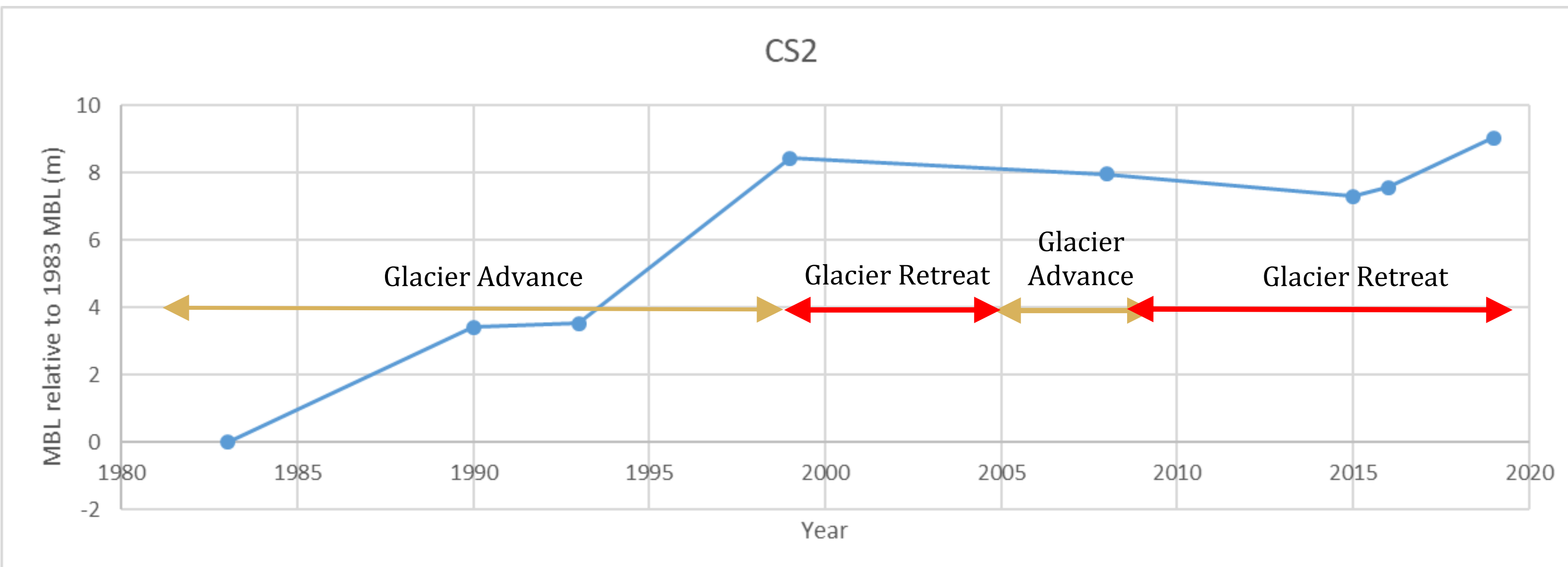
CS2
10
8
6
4
2
0
-2
MBL relative to 1983 MBL (m)
1980
1985
1990
1995
2000
2005
2010
2015
2020
Year
Glacier Advance
Glacier Retreat
Glacier Advance
Glacier Retreat

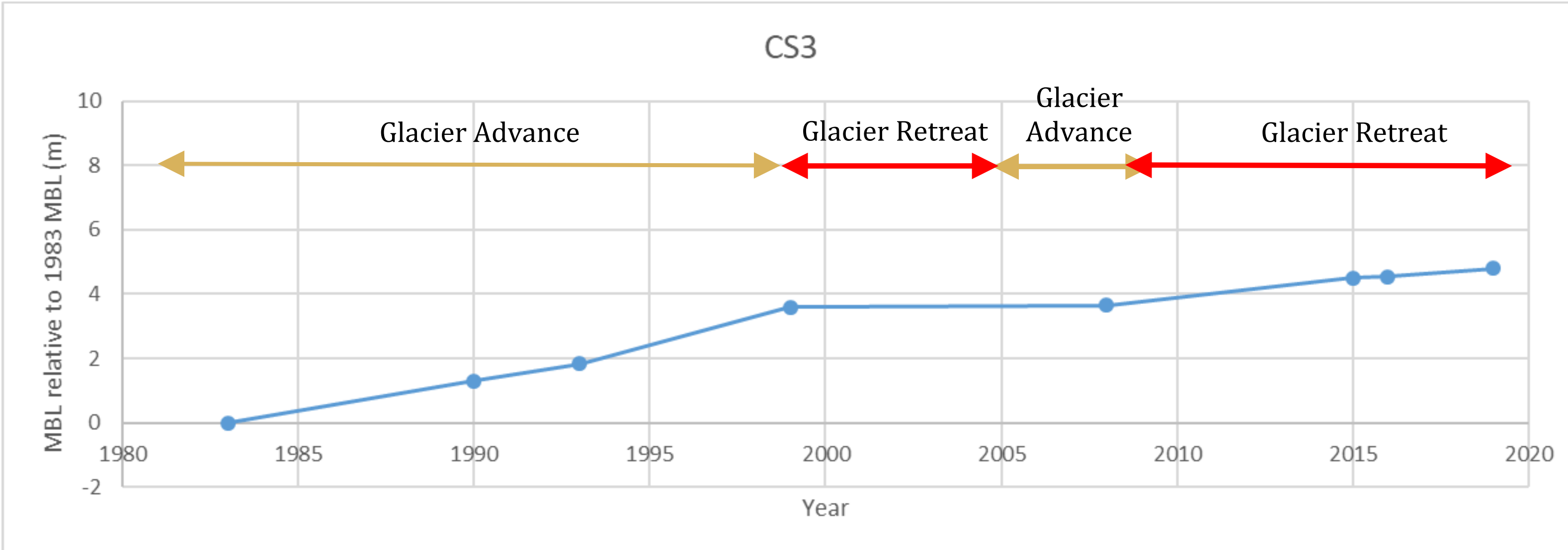
CS3
MBL relative to 1983 MBL (m)
Year
Glacier Advance
Glacier Retreat
Glacier Advance
Glacier Retreat
10
8
6
4
2
0
-2
1980
1985
1990
1995
2000
2005
2010
2015
2020

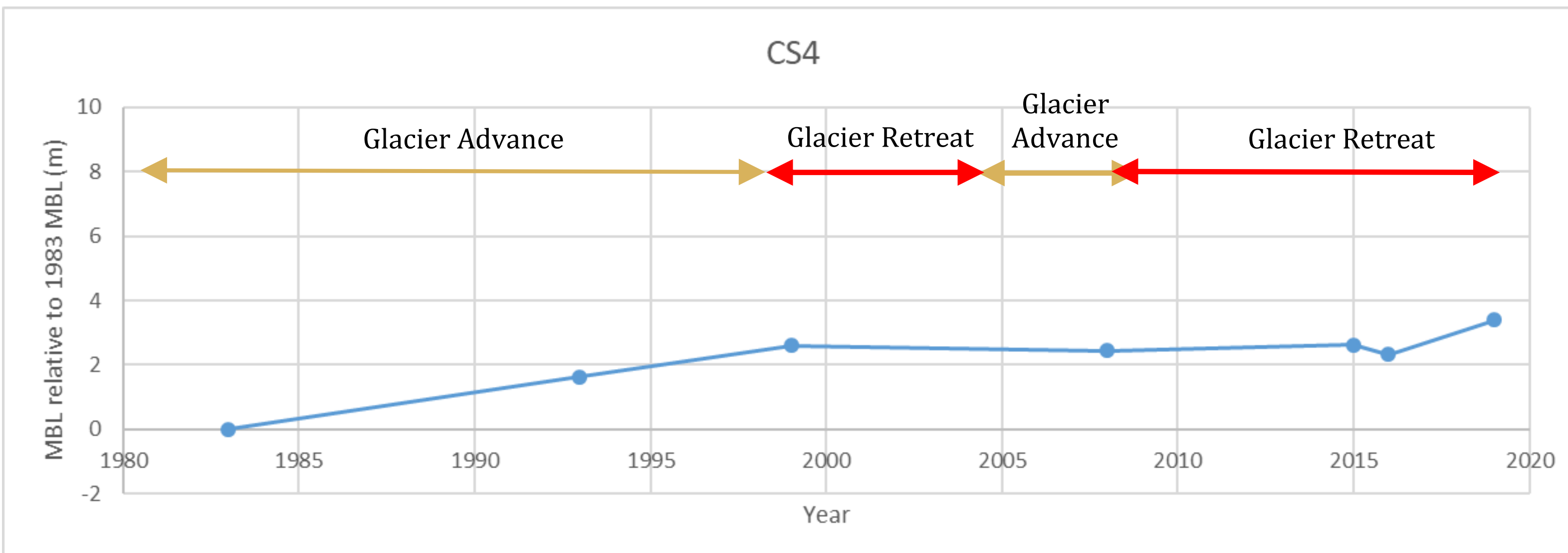
CS4
MBL relative to 1983 MBL (m)
Year
Glacier Advance
Glacier Retreat
Glacier Advance
Glacier Retreat
10
8
6
4
2
0
-2
1980
1985
1990
1995
2000
2005
2010
2015
2020

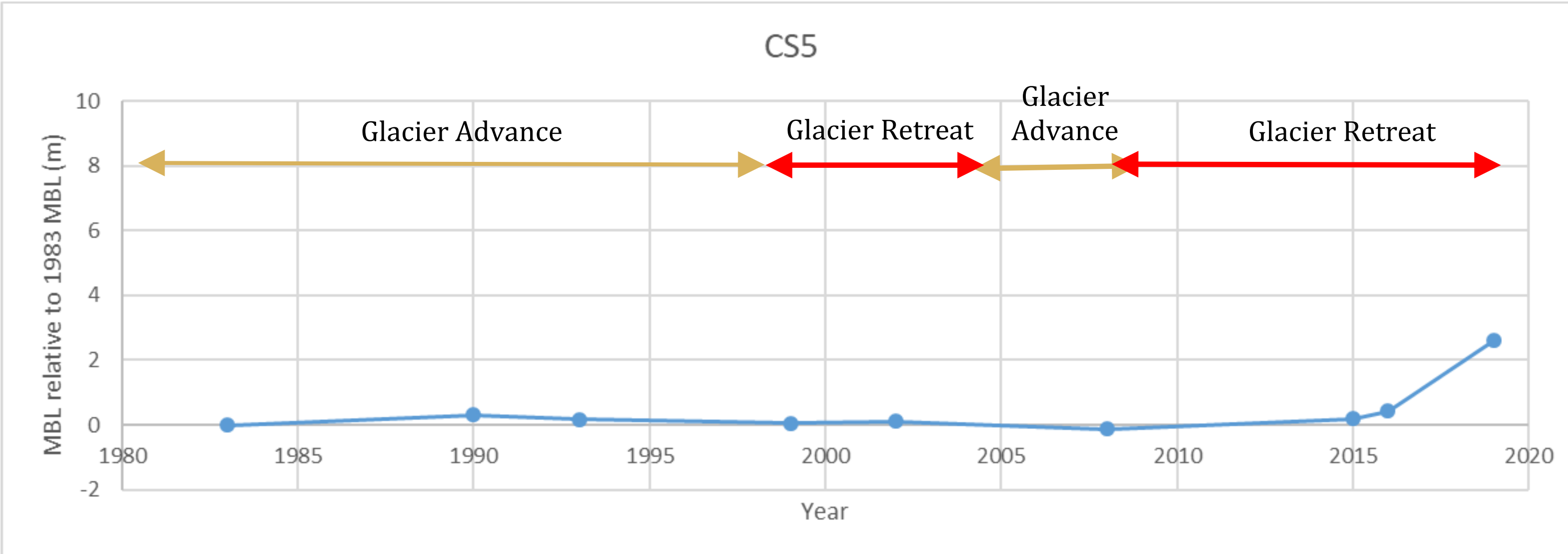
CS5
Glacier Advance
Glacier Retreat
Glacier Advance
Glacier Retreat
MBL relative to 1983 MBL (m)
10
8
6
4
2
0
-2
1980
1985
1990
1995
2000
2005
2010
2015
2020
Year

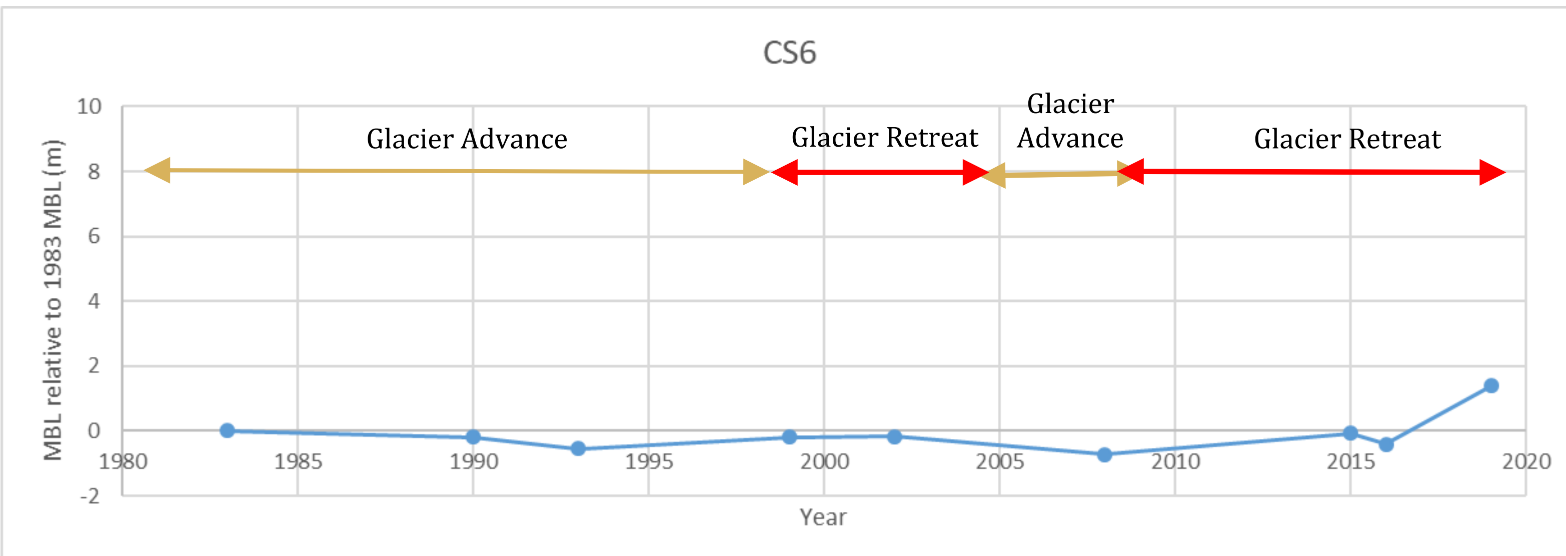
CS6
Glacier Advance
Glacier Retreat
Glacier Advance
Glacier Retreat
MBL relative to 1983 MBL (m)
10
8
6
4
2
0
-2
1980
1985
1990
1995
2000
2005
2010
2015
2020
Year

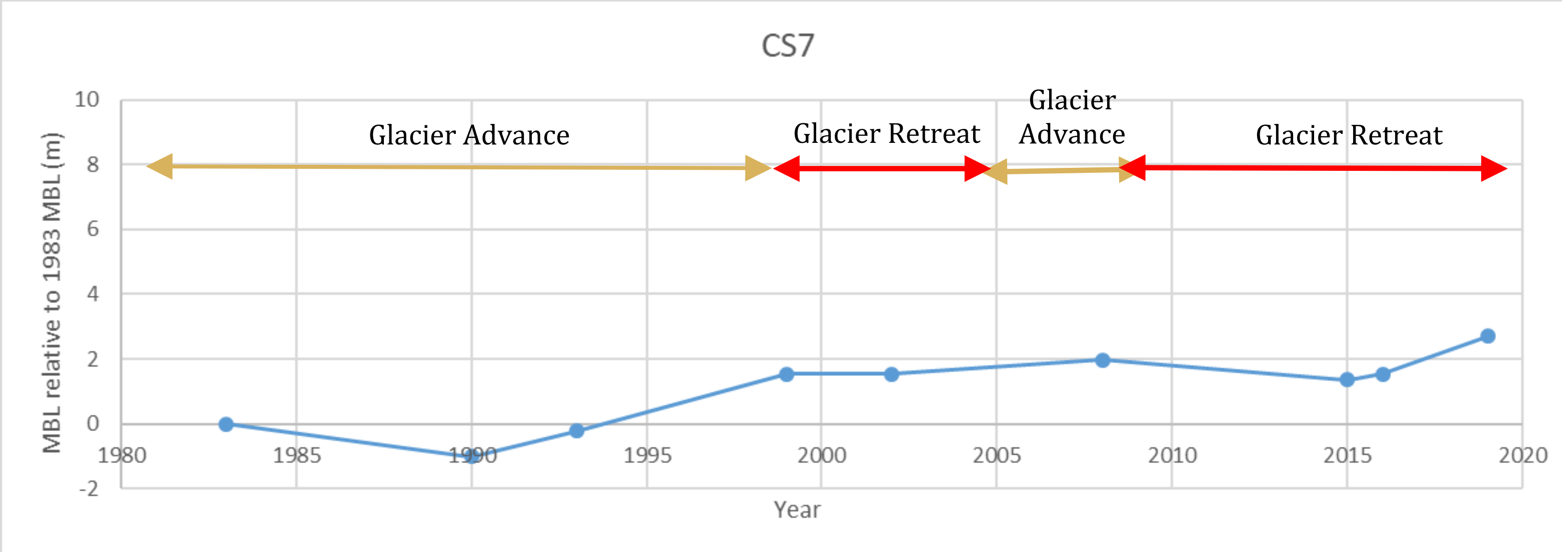
CS7
Glacier Advance
Glacier Retreat
Glacier
Advance
Glacier Retreat
MBL relative to 1983 MBL (m)
10
8
6
4
2
0
-2
1980
1985
1990
1995
2000
2005
2010
2015
2020
Year

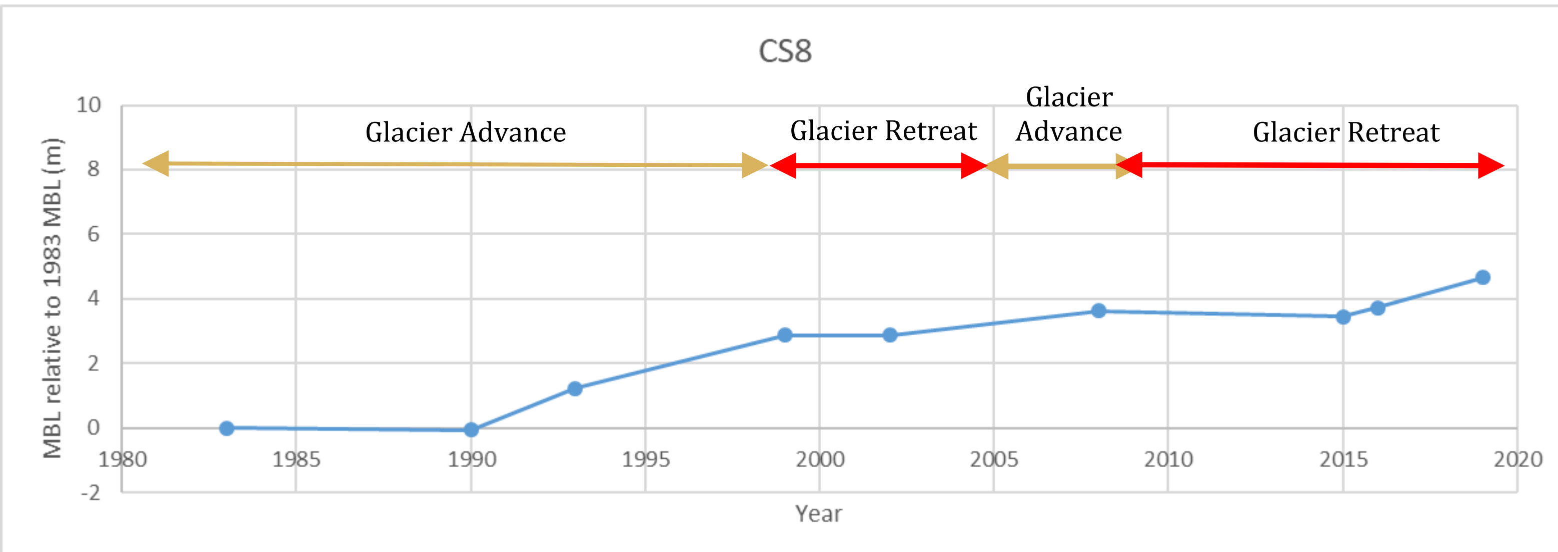
CS8
Glacier Advance
Glacier Retreat
Glacier
Advance
Glacier Retreat
MBL relative to 1983 MBL (m)
10
8
6
4
2
0
-2
1980
1985
1990
1995
2000
2005
2010
2015
2020
Year

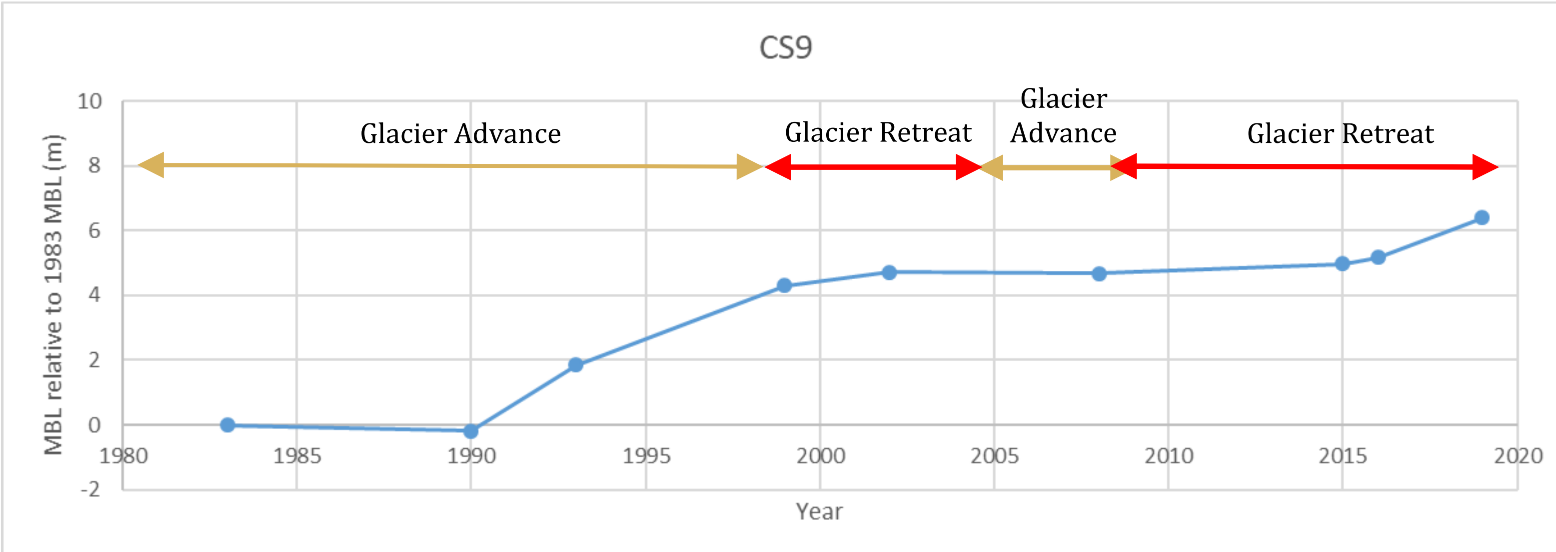
CS9
Glacier Advance
Glacier Retreat
Glacier Advance
Glacier Retreat
MBL relative to 1983 MBL (m)
10
8
6
4
2
0
-2
1980
1985
1990
1995
2000
2005
2010
2015
2020
Year

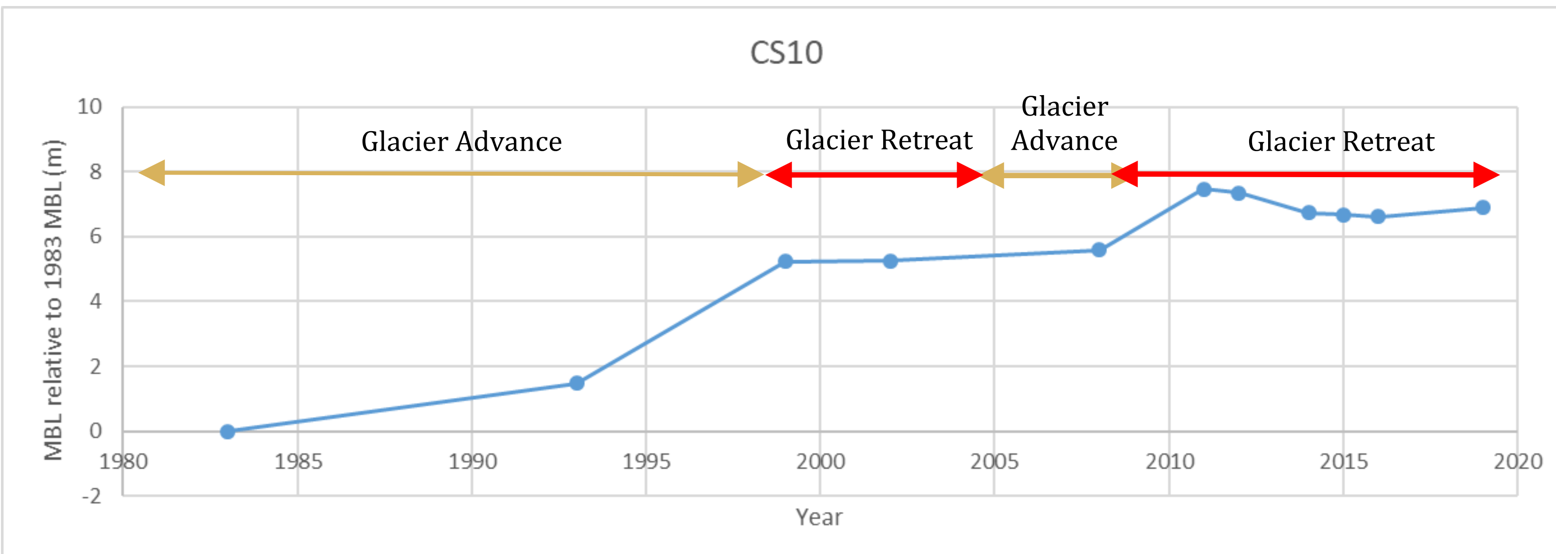
CS10
Glacier Advance
Glacier Retreat
Glacier Advance
Glacier Retreat
MBL relative to 1983 MBL (m)
10
8
6
4
2
0
-2
1980
1985
1990
1995
2000
2005
2010
2015
2020
Year

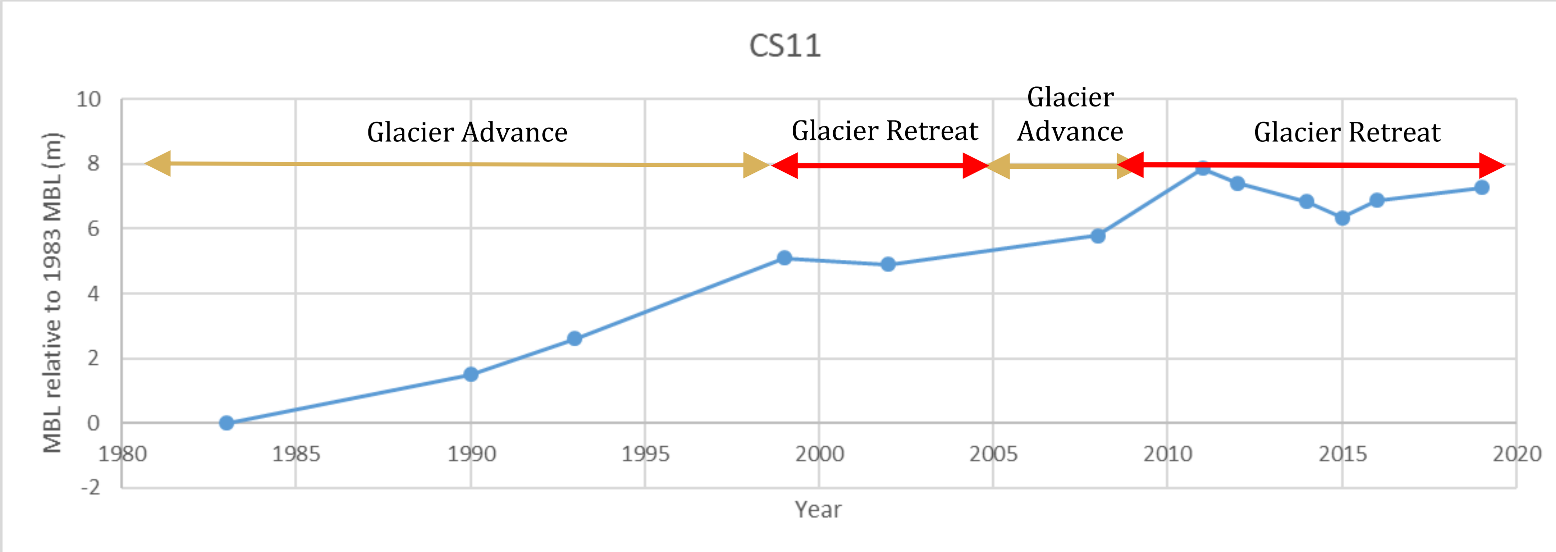
CS11
Glacier Advance
Glacier Retreat
Glacier Advance
Glacier Retreat
MBL relative to 1983 MBL (m)
10
8
6
4
2
0
-2
1980
1985
1990
1995
2000
2005
2010
2015
2020
Year

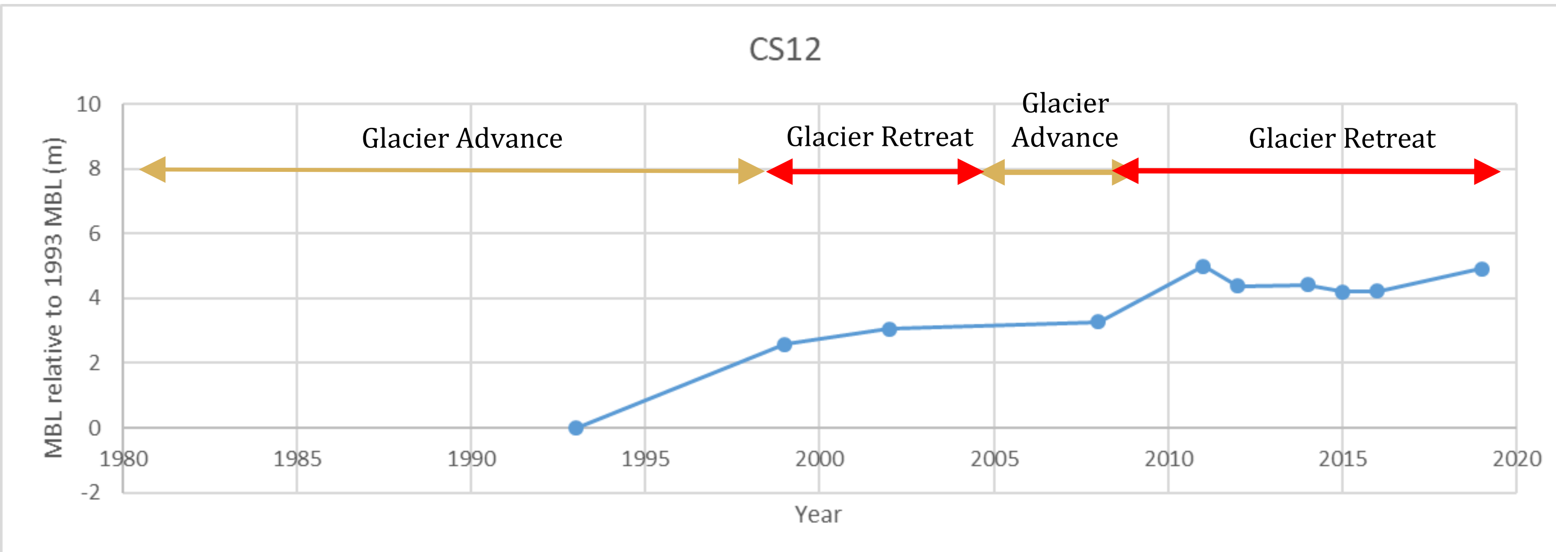
CS12
Glacier Advance
Glacier Retreat
Glacier Advance
Glacier Retreat
MBL relative to 1993 MBL (m)
10
8
6
4
2
0
-2
1980
1985
1990
1995
2000
2005
2010
2015
2020
Year

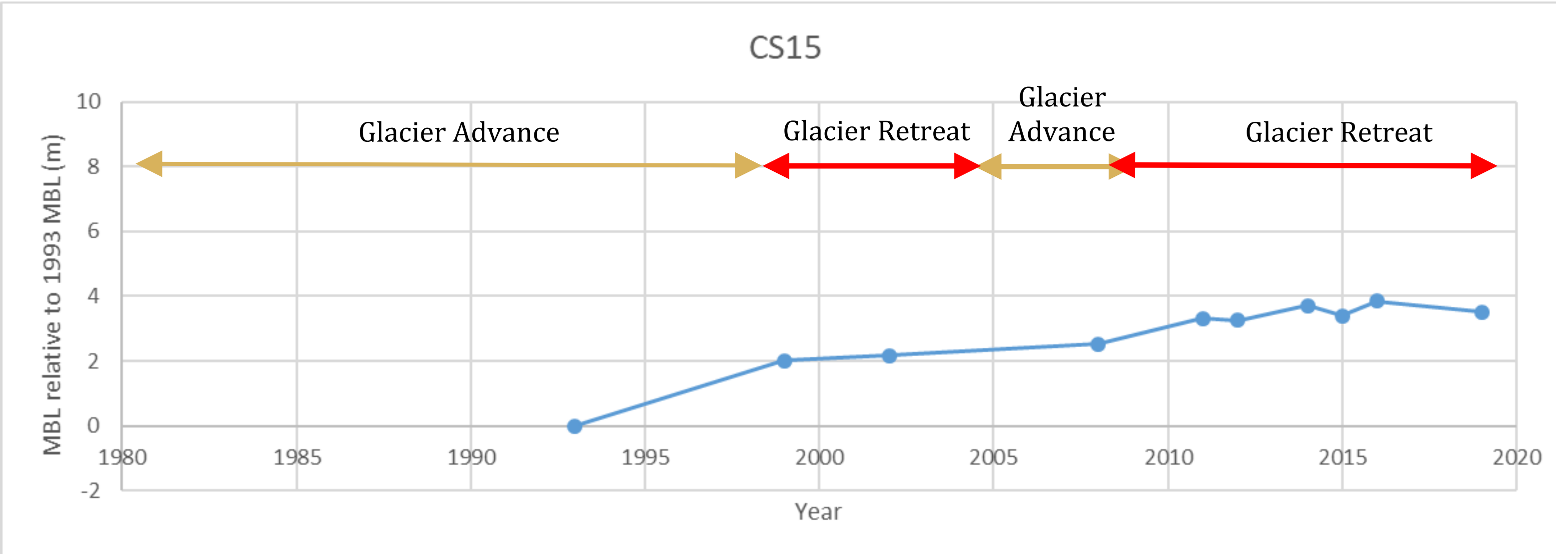
CS15
Glacier Advance
Glacier Retreat
Glacier Advance
Glacier Retreat
MBL relative to 1993 MBL (m)
10
8
6
4
2
0
-2
1980
1985
1990
1995
2000
2005
2010
2015
2020
Year

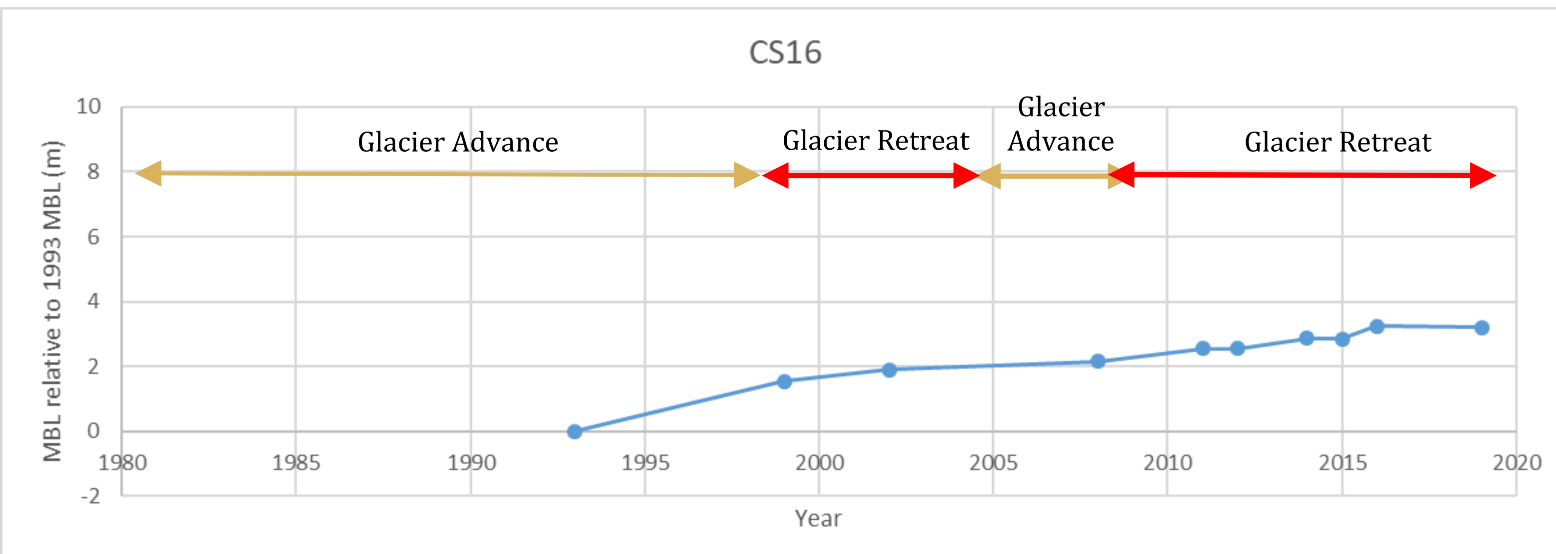
CS16
Glacier Advance
Glacier Retreat
Glacier Advance
Glacier Retreat
MBL relative to 1993 MBL (m)
10
8
6
4
2
0
-2
1980
1985
1990
1995
2000
2005
2010
2015
2020
Year

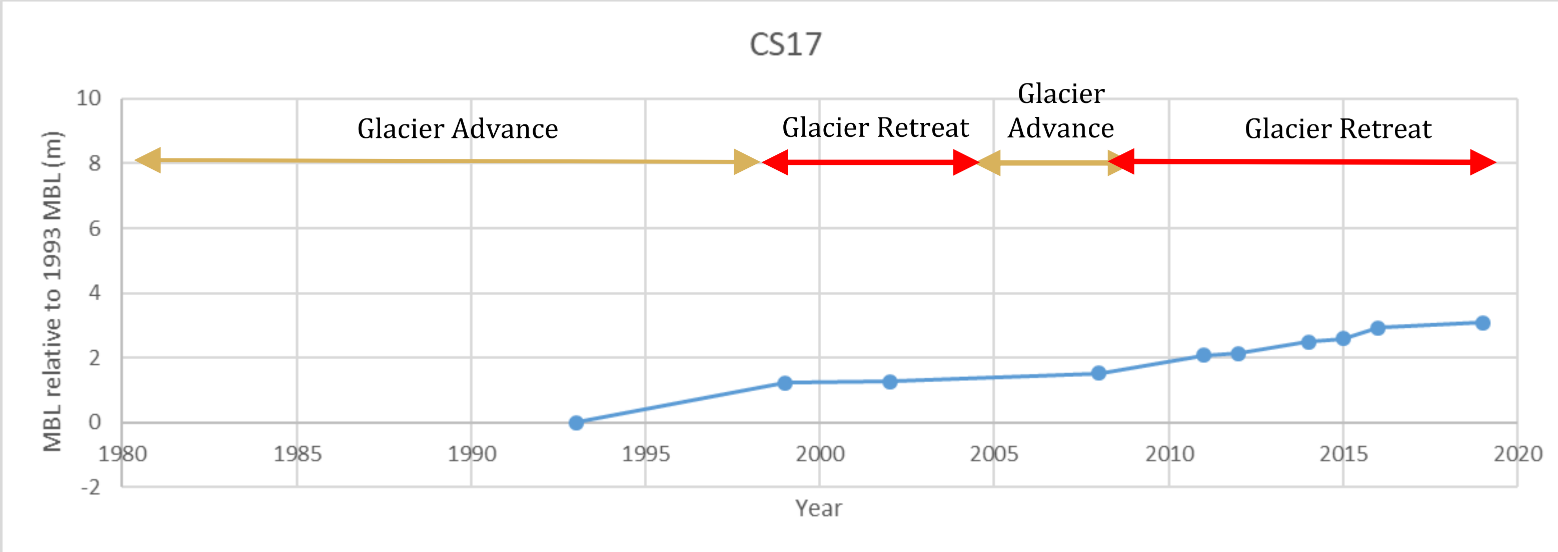
CS17
Glacier Advance
Glacier Retreat
Glacier Advance
Glacier Retreat
MBL relative to 1993 MBL (m)
10
8
6
4
2
0
-2
1980
1985
1990
1995
2000
2005
2010
2015
2020
Year

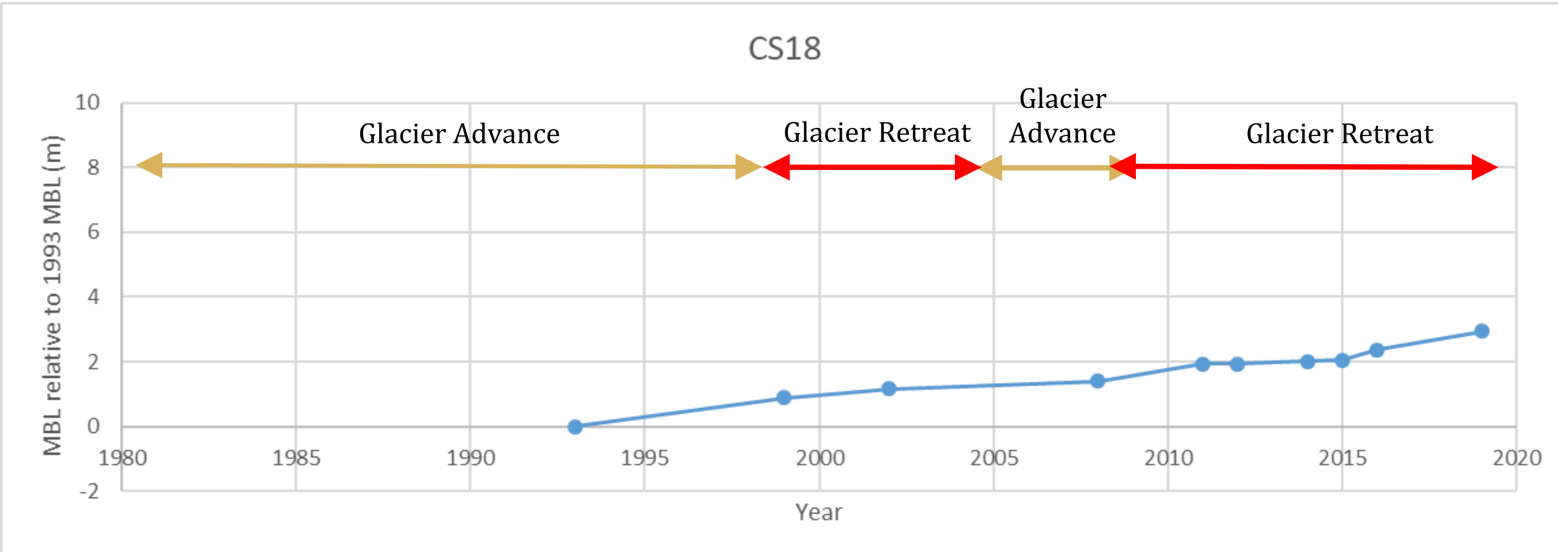
CS18
Glacier Advance
Glacier Retreat
Glacier Advance
Glacier Retreat
MBL relative to 1993 MBL (m)
10
8
6
4
2
0
-2
1980
1985
1990
1995
2000
2005
2010
2015
2020
Year

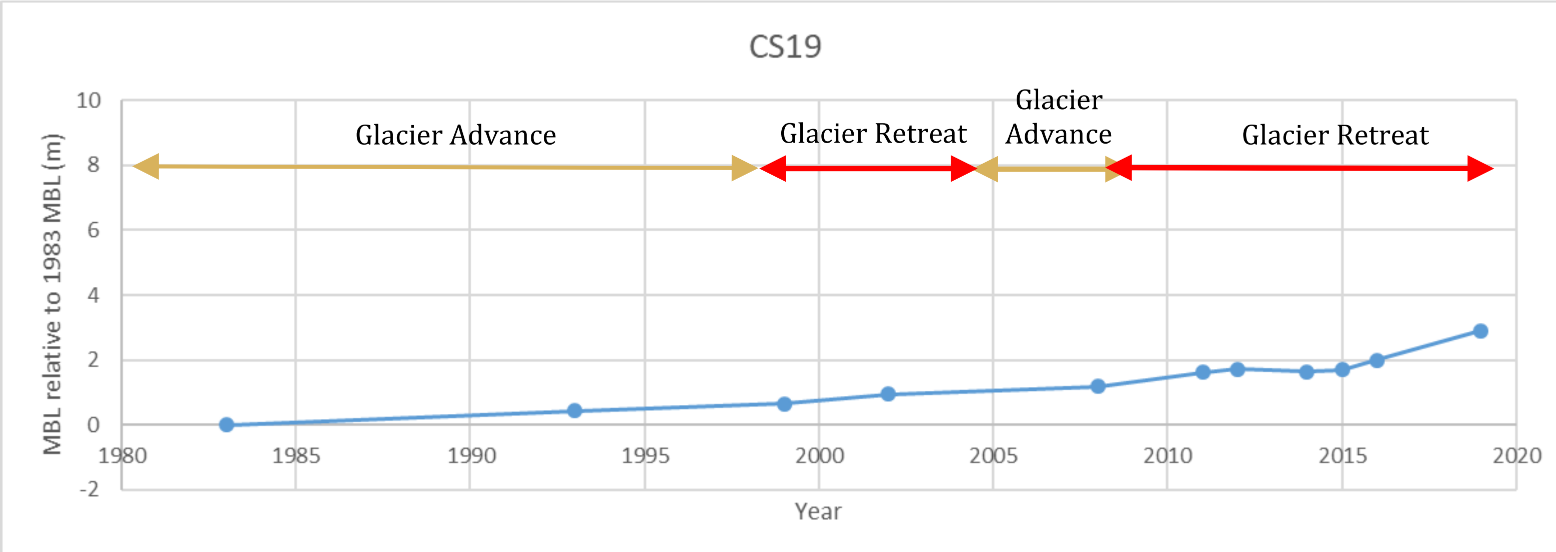
CS19
Glacier Advance
Glacier Retreat
Glacier
Advance
Glacier Retreat
MBL relative to 1983 MBL (m)
10
8
6
4
2
0
-2
1980
1985
1990
1995
2000
2005
2010
2015
2020
Year

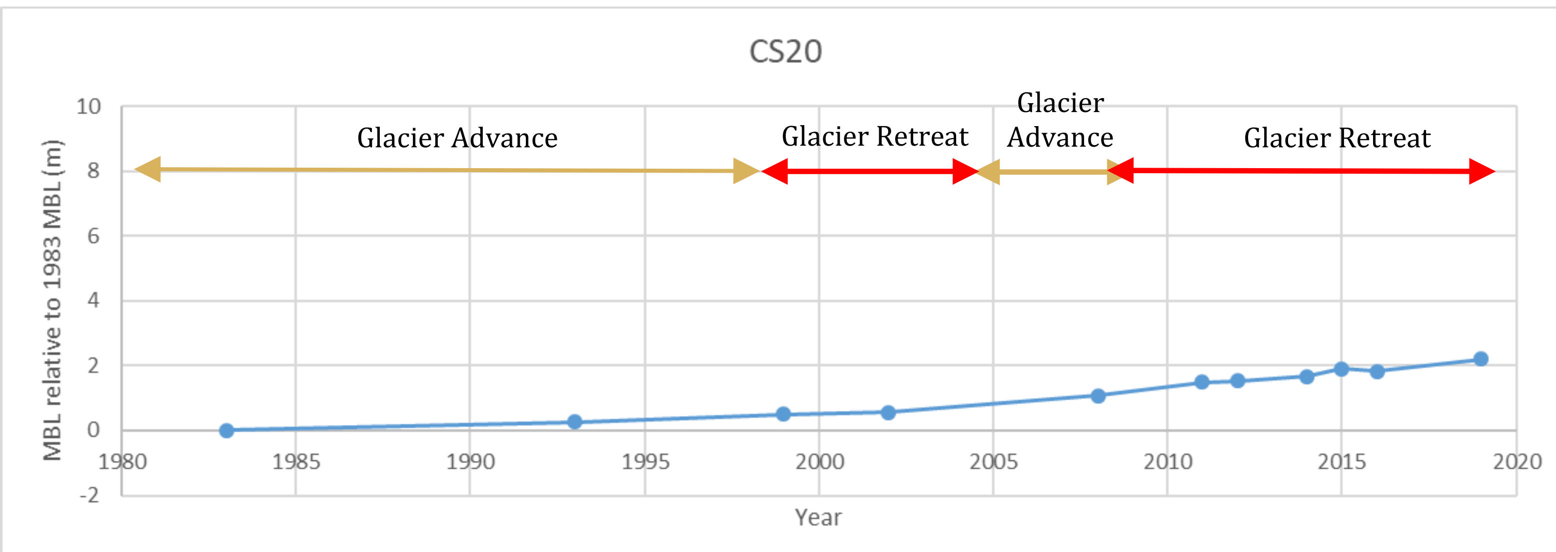
CS20
Glacier Advance
Glacier Retreat
Glacier
Advance
Glacier Retreat
MBL relative to 1983 MBL (m)
10
8
6
4
2
0
-2
1980
1985
1990
1995
2000
2005
2010
2015
2020
Year

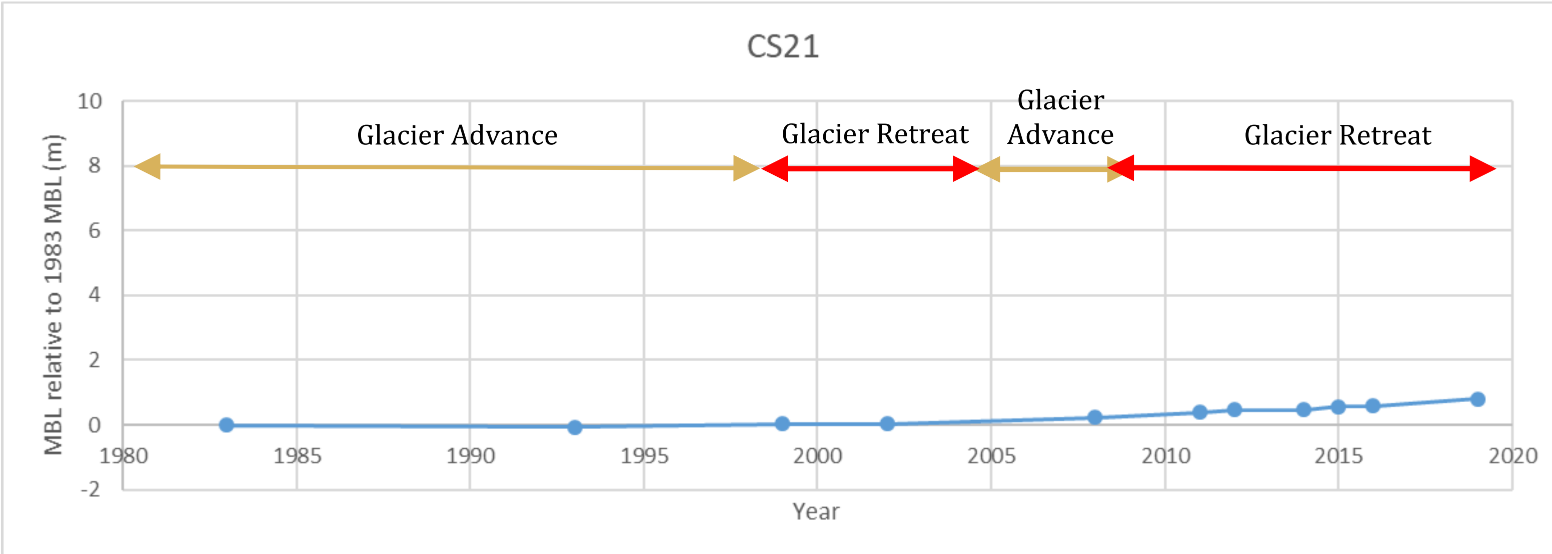
CS21
Glacier Advance
Glacier Retreat
Glacier Advance
Glacier Retreat
MBL relative to 1983 MBL (m)
10
8
6
4
2
0
-2
1980
1985
1990
1995
2000
2005
2010
2015
2020
Year

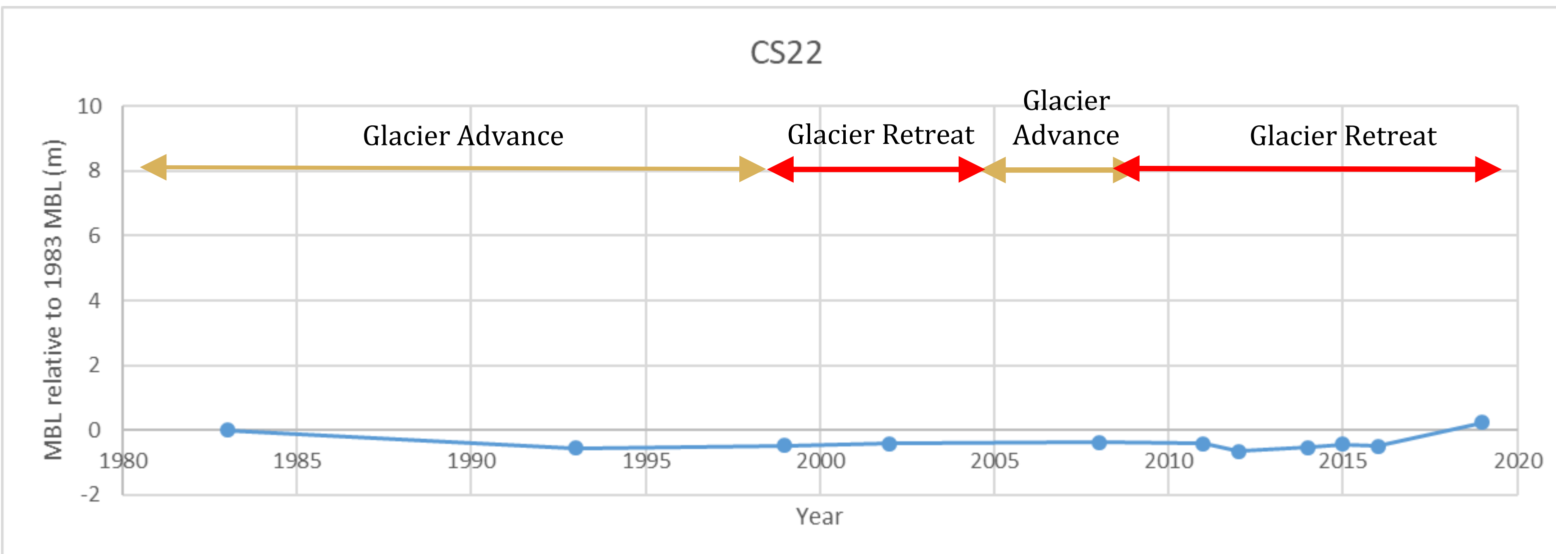
CS22
Glacier Advance
Glacier Retreat
Glacier Advance
Glacier Retreat
MBL relative to 1983 MBL (m)
10
8
6
4
2
0
-2
1980
1985
1990
1995
2000
2005
2010
2015
2020
Year

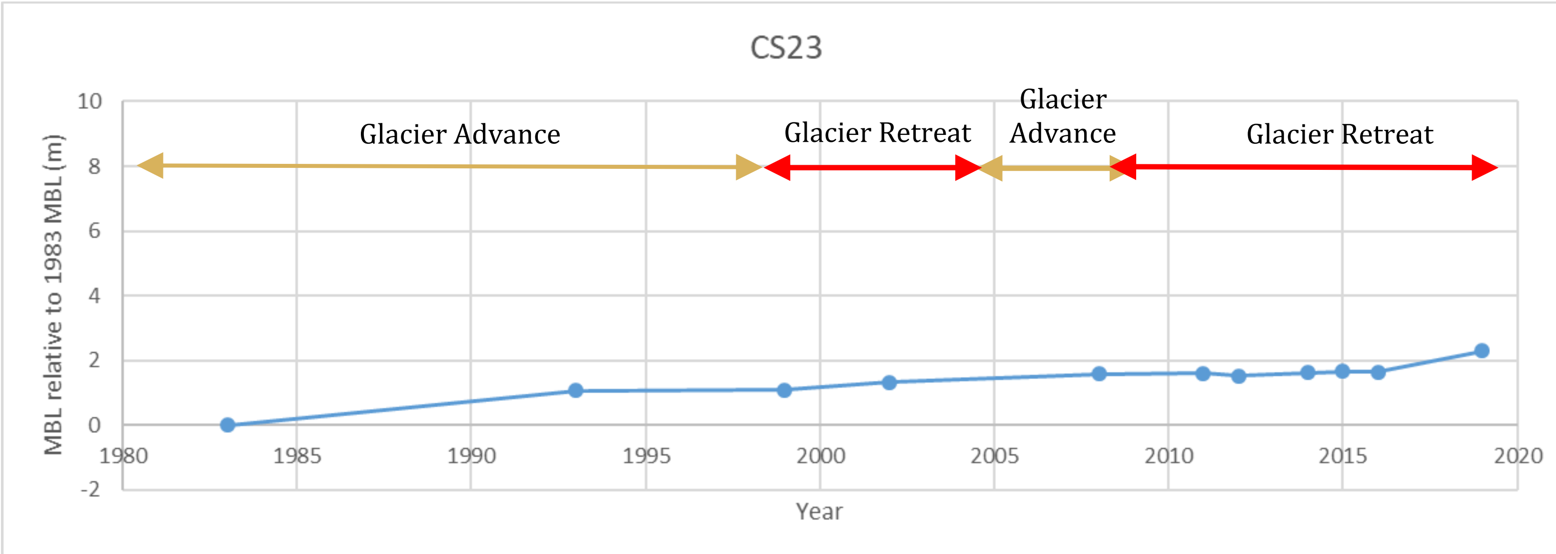
CS23
Glacier Advance
Glacier Retreat
Glacier Advance
Glacier Retreat
MBL relative to 1983 MBL (m)
Year
10
8
6
4
2
0
-2
1980
1985
1990
1995
2000
2005
2010
2015
2020